ELECTRON SPIN RESONANCE STUDIES OF CALCIUM-TREATED HUMAN ERYTHROCYTES AND ERYTHROCYTE GHOSTS

By

DOROTHY ADAMS BERTLER

Bachelor of Arts
St. Mary's University
San Antonio, Texas
1967

Master of Science
University of Puget Sound
Tacoma, Washington
1973

Submitted to the Faculty of the Graduate College
of the Oklahoma State University
in partial fulfillment of the requirements
for the Degree of
MASTER OF SCIENCE
July, 1975

ELECTRON SPIN RESONANCE STUDIES OF CALCIUM-TREATED HUMAN ERYTHROCYTES AND ERYTHROCYTE GHOSTS

Thesis Approved:

Thesis Adviser

Dean of the Graduate College

ACKNOWLEDGMENTS

The author wishes to express her appreciation for guidance received from Dr. Kermit L. Carraway, her major adviser. Appreciation is also expressed to the other committee members, Dr. R. E. Koeppe and Dr. H. Olin Spivey, for their assistance in final manuscript preparation.

Acknowledgment must also be given to Dr. William J. Leivo, Mark E. Markes and Trecia Markes of the Physics Department for their invaluable assistance. A hearty thanks is extended to my typist, Charlene Fries, and to those of the graduate faculty who have patiently answered many questions. But most of all, the author must humbly thank her patient family for bearing with her through this effort.

TABLE OF CONTENTS

LIST OF TABLES

LIST OF FIGURES

Figure Page

LIST OF ABBREVIATIONS

ESR	Electron Spin Resonance
NMR	Nuclear Magnetic Resonance
PS	Phosphatidyl Serine
PC	Phosphatidyl Choline
NMS	Nitroxymethyl Stearate
BSA	Bovine Serum Albumin
RBC	Red Blood Cell
MSL	Maleimide Spin Label

CHAPTER I

INTRODUCTION

Recently, the use of ESR and nitroxide-bearing spin labels has found wide applicability in examination of biological systems. While this method of examination is still essentially in its infancy, there are several excellent reviews of the area (1-10). The phenomemon of ESR is based upon the following fundamental properties of the electron:

1. Mass.
2. Charge.
3. Spin or intrinsic angular momentum.

When an electron is introduced into a uniform magnetic field of strength H, the electron magnetic dipole produced by the spinning of the electron will precess about the axis of the field (Larmour precession). This precession has a finite frequency, omega, given by

$$\omega = \gamma H \tag{1}$$

where γ is the gyromagnetic ratio of the dipole, or more specifically, the ratio of the magnetic moment to the angular momentum. The magnetic energy of this interaction, E, is given by

$$E = \mu_s H \cos\theta \tag{2}$$

where μ_s is the magnetic dipole, H is the external field, and θ is the angle between the axis of the dipole and the field. Since an electron possesses a spin, S, of $\frac{1}{2}$, there can be only two values of θ. These angles are 35° 15" and 144° 45" (11). If one has two electrons

spinning in the same orbit, according to the Pauli exclusion principle, the spins would be opposed, and therefore the magnetic moments will cancel one another out. In the case of a free radical, which is defined in general for spectroscopic examination as a species containing a net spin, there can be two degenerate energy levels of $+\frac{1}{2}$ and $-\frac{1}{2}$. When a magnetic field is applied, these energy levels are split into Zeeman lines with two energy states. The higher energy state is that in which the electron has aligned itself antiparallel to the field and has an energy given by $-g_e\beta H$, where g_e is the g-matrix (discussed later) for a single electron, and has a value of 2.0023, β is the Bohr magneton and H is the applied field strength in Gauss.

The relationship between magnetic field, H, and required frequency, ν, for a given resonance condition is:

$$\Delta E = h\nu = g_e\beta H,$$

where ΔE is the difference in energy levels, and ν is the frequency of incident radiation. During an ESR experiment, microwave energy is absorbed by the sample. Many factors influence the character of the absorption giving detail to the spectrum recorded. The absorption is basically due to electrons contained within the sample, and the most simple sample which could be considered is an infinite potential well which encloses an electron. However, a macroscopically detectable absorption could occur only if many electrons were considered. In order to achieve this, the macroscopic sample could be considered to be composed of many such potential wells. Each of the electronic charges has an internal motion similar to the rotation of a macroscopic

body about some axis; this motion is the basis for the energy absorption.

If a magnet is exposed to a magnetic field with magnetic induction $\vec{H}$, its energy can be described through the magnetic moment $\vec{\mu}$ associated with it. If the energy of the interaction is W, then

$$W = -\vec{\mu} \cdot \vec{H} \tag{4}$$

and the energy varies with the orientation of the magnet with respect to the field $\vec{H}$. Indeed, this may be related to anisotropic motion within a molecule (orientation dependent) in that the magnitude of the induced field depends on the orientation of the molecule itself with respect to the applied field.

The magnetic moment of a charged rotating body is proportional to its rotational angular momentum A:

$$\vec{\mu} = \gamma \vec{A} \tag{5}$$

where γ is again the gyromagnetic ratio. Equation (4) can be combined with Equation (5) using some rules of quantum mechanics for free electrons. In quantum mechanics, angular momentum $\vec{A}$ is expressed in units of Planck's constant h over 2π, designated as $\hbar$, which has a value of 1.05×10^{-34} Joule-sec. Magnetic moment is expressed in units of the Bohr magneton, β, which has a value of 9.27×10^{-28} Joule/Gauss. Also, a free electron is known to assume only two orientations in a magnetic field, as previously indicated; therefore:

$$\vec{A} \cdot \vec{H} = \pm \frac{1}{2} \hbar H \tag{6}$$

The gyromagnetic ratio can be expressed in terms of β and $\hbar$ as

$$\gamma_e = g_e \frac{\beta}{\hbar} \tag{7}$$

where g_e is dimensionless in the case of a free electron, and has a

measured value of 2.00232. The energy can now be written as

$$W = \pm \frac{g_e \beta H}{2} \tag{8}$$

When the energy of the incident microwave photons is equal to the difference in energy between the two orientations, the magnetic field component of the photon can induce a change in the spin orientation. In the process the photon is either absorbed, as in the transition from low to high energy, or it stimulates the emission of a second photon, as in the transition from high to low energy. The energy of the incident photons of frequency v is hv, and the separation in electron energy levels is $g_e \beta H$. Therefore, free electrons can interact with the microwave radiation field when the equation

$$h\nu = g_e \beta H$$

is satisfied.

Real samples differ in many important ways from a collection of electrons in potential wells (12-14). First, one must consider pairing of electrons. Electrons in atoms and molecules occupy specific spatial regions called orbitals. These orbitals are probably more accurately described as probability distributions describing where the electron is most probably found with respect to a given nucleus. The Pauli exclusion principle, as mentioned before, restricts the number of electrons in an orbital to no more than two with opposing spins. This results in no net magnetic moment for the pair, and they cannot interact with the microwave field. Due to the fact that most, if not all, electrons in a sample are paired, only a small fraction of them contribute to the energy of the absorption as outlined above.

Another consideration is power saturation and relaxation times (15). Power absorption stops when the two energy levels, separated by the action of the magnetic field become equally populated. In this case, since the populations of the two states are equal, just as many photons will interact with low energy unpaired electrons and be absorbed as interact with high energy electrons and stimulate emission of a new photon of the same energy, and no net photons will be absorbed. In this case, the sample is said to be power saturated.

A natural difference in population exists for samples with unpaired electrons. Such "paramagnetic" samples have the unpaired electrons distributed as follows:

$$\frac{N^+}{N^-} = e^{\left[\frac{w^+ - w^-}{KT}\right]} \tag{9}$$

where N^- is the number of unpaired electrons in the lower energy level and N^+ is the number of unpaired electrons in the higher energy level, w^{+}_{-} is the energy value, K is the Boltzmann constant, and T is the absolute temperature.

If this distribution is momentarily disturbed, there is a tendency for it to be restored, since the electrons tend to interact with their surroundings. It is through the forces of this interaction that the energy absorbed by the electrons from the microwave field is dissipated, allowing a continuous absorption of energy by the sample. However, if these forces are weak and the incident power intense, then the population difference tends to zero, and the sample is said to be power saturated. Partial saturation can occur, and in this case, the population difference is smaller than normal at that temperature, and the absorption of power is less intense.

The ESR spectrum of many samples shows a dependence on molecular orientation with respect to the applied magnetic field (16). If the energy level separation of two spin states is designated by means of a "g-factor" as was done for a free electron, it would be found that this effective g-factor would be given by:

$$g_{eff} = \frac{h\nu}{\beta H_r} \tag{10}$$

where H_r is the field at which the resonance is observed to occur and is dependent on the orientation of the molecule absorbing the microwave photon, and as a result, no single g-factor could be assigned as characteristic of the molecule.

In order to find something which is characteristic of the molecule, the local field at the absorbing electron must be considered. As before, the energy W can be written:

$$W = -\vec{\mu} \cdot \vec{H} \tag{11}$$

However, in a real sample, $\vec{H}$ is often not the applied external field $\vec{H}_a$. The orbital in which the electron travels can contain some orbital angular momentum, and due to its motion about the charged nuclear core, the electron feels an additional magnetic force. The actual field at the electron still depends on the applied field, but only through a transformation matrix $[T_1]$ as:

$$\vec{H} = [T_1]\ \vec{H}_a \tag{12}$$

Now if the electron spin angular momentum $\vec{A}$ is written as

$$\vec{A} = \vec{S}\ h \tag{13}$$

the energy levels can be written as

$$w = -\vec{\mu} \cdot \vec{H} = -g_e\ \beta \vec{S}\quad [T_1]\quad \vec{H}_a \tag{14}$$

since μ and H are known from Equations (4), (5) and (12). It is customary to drop the "applied" notation on the magnetic field, and combine $-g_e$ and $[T_1]$ to obtain what is called the "g-tensor"; g:

$$[g] = -g_e\,[T_1] \tag{15}$$

With these modifications, the energy level becomes:

$$W = \beta \vec{S} \cdot [g] \cdot \vec{H} \tag{16}$$

and the quantum mechanical "spin-Hamiltonian" can be written:

$$\mathcal{H} = \beta \vec{S}_{op} \cdot [g] \cdot \vec{H} \tag{17}$$

by making the formal substitution:

$$\vec{S} \rightleftarrows \vec{S}_{op} \tag{18}$$

The g-tensor can be simplified by a suitable choice of coordinates. If an arbitrary set of axes is defined for a molecule, and all the nine components found by means of an ESR experiment, the g-tensor would be symmetric. This symmetric tensor can be diagonalized by a transformation of axes. The spin Hamiltonian with the g-tensor in diagonal form is:

$$H = \beta(S_{xop}\ S_{yop}\ S_{zop}) \begin{bmatrix} g_{xx} & 0 & 0 \\ 0 & g_{yy} & 0 \\ 0 & 0 & g_{zz} \end{bmatrix} \begin{bmatrix} H_x \\ H_y \\ H_z \end{bmatrix} \tag{19}$$

The g-factor observed at a particular angle of applied H can be found if the three components of the diagonalized g-tensor are known. This is done by writing H in terms of its direction cosines relative to the diagonalization axes:

$$\vec{H} = H \cos\alpha\ \hat{x} + H \cos\beta\ \hat{y} + H \cos\gamma\ \hat{z} \tag{20}$$

Now the energy levels are written:

$$W = \beta \vec{S} \cdot [H^2 \cos^2\alpha\, g_{xx}^2 + H^2 \cos^2\beta\, g_{yy}^2 + H^2 \cos^2\gamma\, g_{zz}^2]^{\frac{1}{2}} \hat{H} \tag{21}$$

and since:

$$\vec{S} \cdot \vec{H} = \pm \frac{1}{2} \tag{22}$$

the measured energy separation is:

$$\Delta E = \beta H [\cos^2\alpha\, g_{xx}^2 + \cos^2\beta\, g_{yy}^2 + \cos^2\gamma\, g_{zz}^2]^{\frac{1}{2}} \tag{23}$$

and the effective g-factor is defined as:

$$g_{eff} = [\cos^2\alpha\, g_{xx}^2 + \cos^2\beta\, g_{yy}^2 + \cos^2\gamma\, g_{zz}^2]^{\frac{1}{2}} \tag{24}$$

The spin Hamiltonian for the system may be related to the g-factor as follows:

$$\mathcal{H} = |\beta|\, \hat{S}\, g\, H + \hat{S}\, T\, \hat{I} + [\text{Electron-Electron Dipole Term}] + [\text{Electron-Electron Exchange Terms}] \tag{25}$$

where g is the g-matrix, H is the laboratory magnetic field, $\hat{S}$ is the electron spin operator, T is the hyperfine matrix, and $\hat{I}$ is the nuclear spin operator.

The hyperfine matrix encompasses the effect of the magnetic moment of the nucleus at the electron. The labels employed in this study show the effect of the ^{14}N nucleus. The ^{14}N nucleus has three possible spin states; that is, the nuclear magnetic field can add to, subtract from, or fail to modify the applied magnetic field. Any sample will contain approximately equal numbers of the label molecule in the three different states, and the result will be three lines in the spectrum instead of one. In addition, this effect depends on the orientation of the

applied field relative to the label molecule. The separation between the three equally spaced lines will vary depending upon molecular orientation. This orientation-dependence, as in the case of the g-factor, can be completely specified by a 3 x 3 matrix, which can be diagonalized by choice of the proper coordinate system for the expression of H, the applied magnetic field. The spin Hamiltonian with hyperfine interaction included takes the form:

$$\mathcal{H} = \beta \hat{\vec{S}} \cdot \overleftrightarrow{g} \cdot \vec{H} + \hat{\vec{S}} \cdot \overleftrightarrow{T} \cdot \hat{\vec{I}} \qquad (26)$$

where $\hat{\vec{I}}$ is the nuclear spin operator. In the case of the nitroxide spin labels, it also happens that the principle coordinate system that diagonalizes g also diagonalizes T. These axes can be determined experimentally because they relate directly to maximum and minimum splittings, as in the case of the g-factor.

The ESR spectra of free radicals depends upon the rate of tumbling, and this is also true for the nitroxide radical (10, 17-19). Examples of different types of nitroxide radicals which have been used as labels in various synthetic bilayer preparations (20-25) as well as in several types of biological membranes (26-31) are given in Figure 1. The line widths of a given ESR spectrum are a measure of anisotropies of the hyperfine interaction and g-factor, and these are increasingly averaged out as the solvent system decreases in viscosity. This phenomenon has been extensively studied for 14_N (2, 25, 17, 32). The nitroxide radical in water shows three distinctly separated lines, appearing equidistant from each other. As the viscosity of the solvent increases, the peak to peak separation of these lines increases, and there is line broadening with concomitant alteration in the peak intensities. The types of information which we may be able to glean from the introduction

Figure 1. Types of Nitroxide Spin Labels Used in Studies of Biomembranes

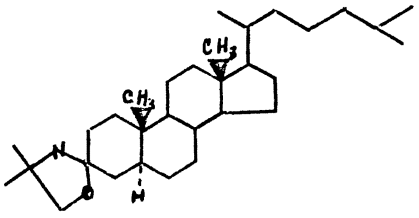

N-oxyl-4', 4'-dimethyloxazolidine derivative of 5α-cholestan-3-one

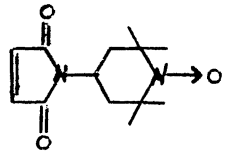

A maleimide label

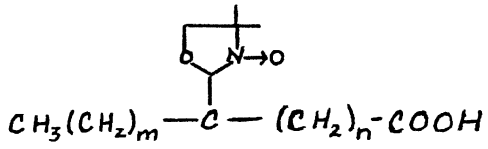

x(m,n); fatty acid labels

of a nitroxide label into a biological membrane are as follows:

1. Since the electron spin resonance spectra are sensitive to the rate at which the label is able to reorient, the degree of mobility permitted by the immediate environment may be evaluated.

2. The g-factor and hyperfine splitting vary with the polarity of the solvent; therefore we may examine the polarity of the label environment.

3. Since the area under the absorption response is proportional to the total number of unpaired spins in the samples, assuming no saturation is taking place, one can theoretically quantitate the amount of probe present in the samples.

So, by following the changes of the ESR spectrum of the free radical in the free and bound states, we can deduce information about the environment close to the binding site.

Nitroxides are stable, relatively inert, and give sharp, well resolved spectra, sensitive to the molecular environment. They have the general form:

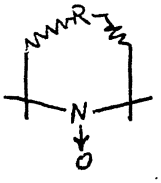

in which there is an odd electron, localized almost entirely on the -N-O group and exhibiting magnetic hyperfine interaction, containing both isotropic and anisotropic components, with the nitrogen nucleus. If the nitroxide radical is present in low concentrations in aqueous or nonviscous solvent, the spectrum observed is three equally spaced lines of approximately equal height. This is due to the fact that the nitrogen nucleus can also be aligned parallel, antiparallel, or

perpendicular to the laboratory magnetic field. The electron then experiences the sum of the external field and three different local magnetic field values from the nitrogen nucleus, and each of these latter field values gives rise to a line in the absorption spectrum. As shown below, the spectra are exhibited as first derivatives of the absorption spectrum instead of Lorentzian lines (16).

The spectrum of a labeled sample includes the effects of label motion and random orientation of these rapidly moving labels. Fig. 2a shows the general outline of an absorption spectrum of a sample with various label orientations. The spectrum is the result of superimposing the lines of the three-line spectra (Fig. 2b) for each of the orientations present. For certain molecular orientations, the splitting is maximum, and only this orientation will contribute to the extreme high and low field portions of the spectrum. This separation often called $T_{||}$, can be obtained by a measure of the overall spectrum width. Most often the spectrum is recorded as the approximate first derivative of the absorption as shown in Fig. 2c, and in this case, we would measure $T_{||}$ as shown in Fig. 3.

In a similar fashion, the separation marked as $T_{\perp}$ can be attributed to those molecules oriented so that a minimum splitting results. The rationale for this choice as well as the choice for the $T_{||}$ measurement can be seen by comparison of the first derivative curve, Fig. 2c, with the absorption curve, Fig. 2a.

There are several parameters which may be used to interpret changes in biological membranes as monitored by spin-label techniques. In our experiments we have measured the change in field separation between high and low fields which corresponds to $2T_{||}$ and $T_{\perp}$ (Fig. 3),

(a) Idealized absorption spectrum

(b) First derivative presentation of the spectrum (a)

(c) Absorption spectrum of maleimide label in 310 mOsM, phosphate, pH 7.4

(d) Maleimide label in 310 mOsM phosphate buffer, pH 7.4, ambient temperature, first derivative presentation

Figure 2. Types of Spectral Representations

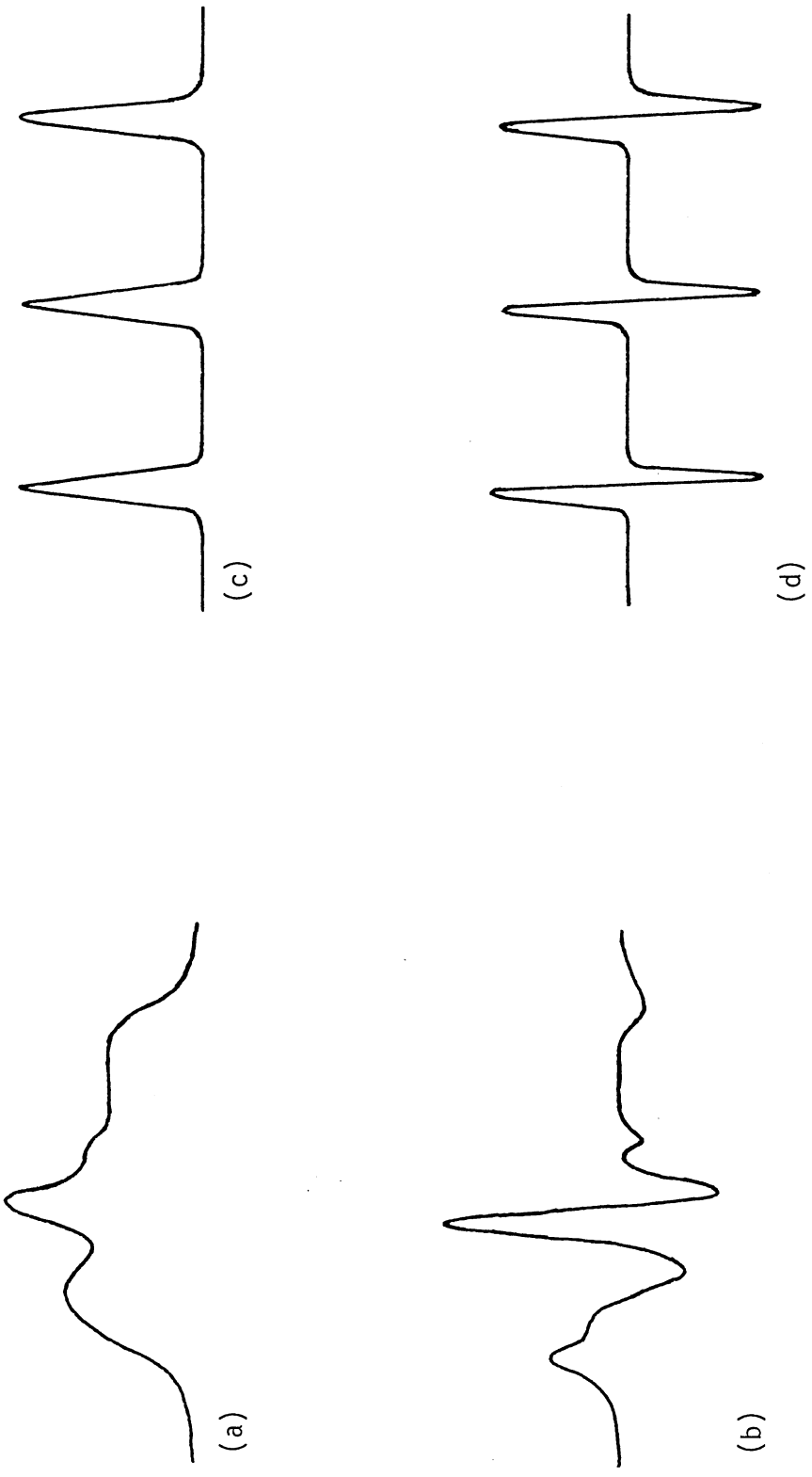
(a)
(b)
(c)
(d)

both of which are components of the motionally averaged hyperfine tensor of nitrogen. As the viscosity of the environment increases and approaches a rigid glass spectrum, the field separation, or $2T'_{\parallel}$, increases. There is a shift in the splitting of the lines and line broadening, as shown by increases in $T'_{\perp}$. These spectral parameters characterize the rigidity with which the label is held. Changes in $T'_{\parallel}$ and $T'_{\perp}$ also indicate a change in the extent of the partial motional averaging in a given sample. McConnell (16) has related changes in $T'_{\parallel}$ to the mean angular deviation of the hydrocarbon chain in the vicinity of the nitroxide label from the axis of symmetry of the rotation of the chain. For lipid hydrocarbon chains, this is simply a measure of the average angular deviation of the molecular axis from the principal axis, perpendicular to the membrane at the nth methylene on the chain. The more rigid the environment, the more restricted the fatty acid chain becomes and, therefore, the smaller the mean angular deviation. This is of particular significance when dealing with stearic acid spin labels in which the nitroxide group is rigidly bound to the stearic acid chain through a spirane linkage. The nitroxide group then accurately reflects the motion of the hydrocarbon chain. The equation expressing the relationship between this angle, θ, and $T_{\parallel}$ is:

$$\langle \cos^2 \theta \rangle = \left(\frac{T'_{\parallel} - T'_{\perp}}{T_{\parallel} - T_{\perp}} \right) \qquad (27)$$

where $T_{\parallel}$ and $T_{\perp}$ refer to the hyperfine tensor parameters measured for the same nitroxide label fixed in a rigid crystal structure, and $T'_{\parallel}$ is the effective parallel hyperfine component resulting from motional averaging. The values used for $T_{\perp}$ and $T_{\parallel}$ are taken from McConnell

et al. (16), as applied by Butterfield et al. (33). These values are based on measurements on cholestane label in a cholesterol chloride crystal.

Order within the membrane is also often characterized by the order parameters, S, which may be defined in terms of the mean angular deviation as follows:

$$S = \frac{1}{2}\left(3\langle\cos^2\theta\rangle - 1\right) \tag{28}$$

S can also be expressed directly in terms of $T_{\perp}'$ and $T_{||}'$:

$$S = \left(\frac{T_{||}' - T_{\perp}'}{T_{||} - T_{\perp}}\right)\left(\frac{a_{nxl}}{a_n'}\right) \tag{29}$$

where the factor (a_{nxl}/a_n') is a solvent polarity correction employed when the parameters are measured under differing polarity conditions. In this case, a_{nxl}' is the coupling constant for the label in a crystal, and a_n' is the coupling constant for the label in the sample. Being directly dependent upon the square of the cosine of the mean angular deviation, the order parameter also changes with alteration of the viscosity of the medium. In short, S is found to decrease as a direct consequence of decreases in $\langle\cos^2\rangle$. By definition, S is bounded between 1, for a completely ordered label (stationary), and 0 for a label undergoing rapid isotropic motion.

Since the extreme high and low field region of the spectrum is enhanced during limited motion and the center region is enhanced during more isotropic motion, relative peak intensities of these two regions can be used to quantitate changes in molecular motion. Verma, et al. (34) have used this method in the examination of the effects of melittin on the erythrocyte membrane. The peaks are labelled in Fig. 3. As the

Figure 3. Typical Spectra of Labeled Erythrocytes

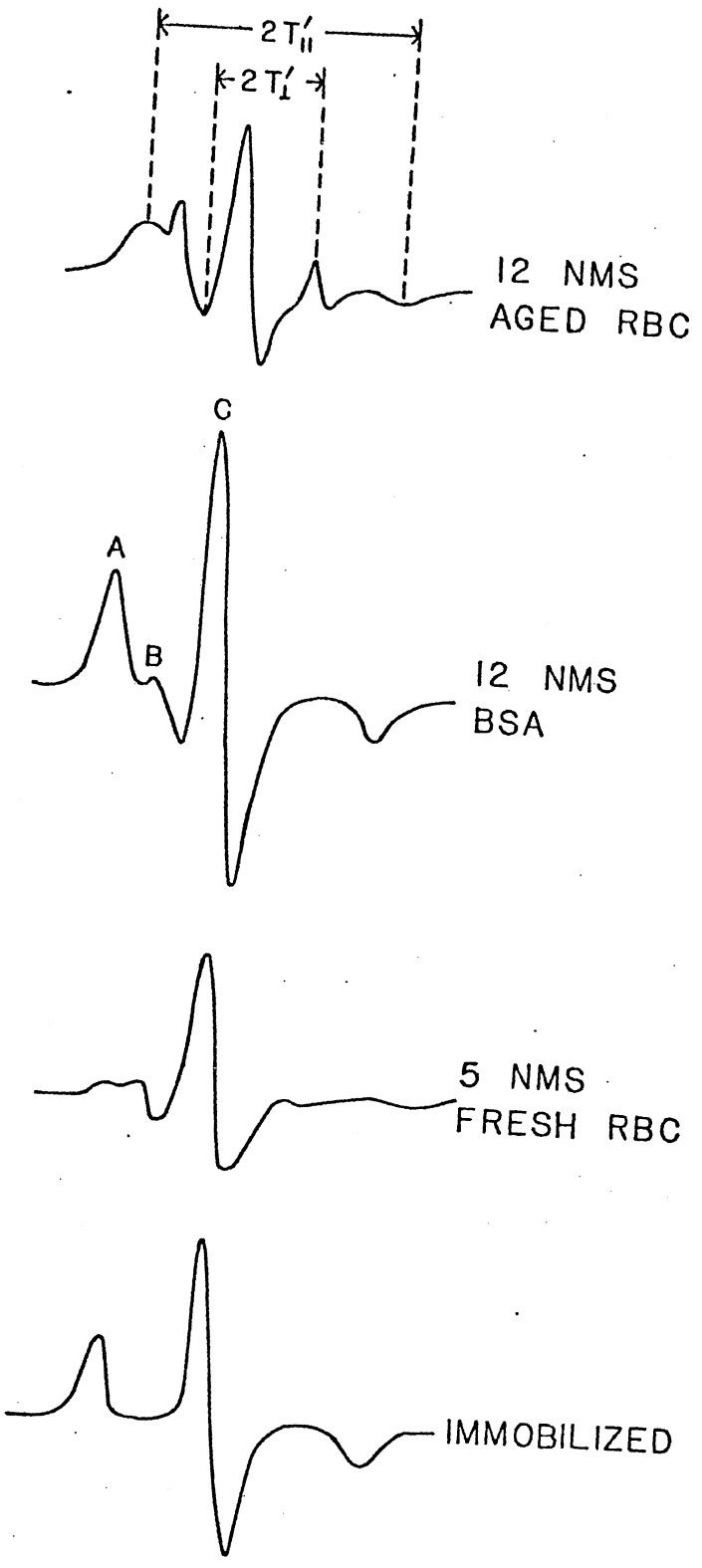
2T''II
2T'I
12 NMS
AGED RBC
C
A
B
12 NMS
BSA
5 NMS
FRESH RBC
IMMOBILIZED

ratio of b/c approaches 1, there is a perfect ordering of the long axis of the probe with respect to the membrane. A decrease in the intensity of b, then, indicates a disordering of the long axis and a decrease in the ratio, with an increase in mobility.

The anisotropic N^{14} hyperfine coupling constant, a'_n, may be calculated from measurements of $2T'_{11}$ and $2T'_{\perp}$ by the equation:

$$a_n = \frac{1}{3}(2T'_{\perp} + T'_{11}) \tag{30}$$

This coupling constant shows a small dependence on the polarity of the solvent, ranging from 14.1 Gauss in hexane to 15.1 in water (33). It follows that it will also show a dependence on the polarity of the environment of the nitroxide in the membrane.

The existence in many, if not all, membrane systems of a bilayer (35-42) has been demonstrated by comparison of spectra from biological membrane systems with those from synthetic systems. The fluidities of these bilayer regions differ significantly, with the erythrocyte membrane being less rigid than viral membranes, and more rigid than nerve cell membranes (30, 36, 39). In general, lipid labels are more useful in examining polarity within the bilayer, and are more easily incorporated. Interpretive problems may arise due to the fact that spin-labeled hydrocarbons may be sterically unable to participate in normal lipid-protein interactions and might be sterically excluded from highly ordered regions of the membrane. Evidence against this is the biosynthetic incorporation of these labels into mitochondria of Neurospora crassa (43), mycoplasma (41), and transformed cells (44).

Phospholipids and cholesterol are essential to structure and function of biological membranes. The variation from cell to cell in

proportions of these and other membrane components, as well as variation in fatty acid chains on phospholipids may dictate functional properties such as permeability of a given membrane. Cholesterol and water affect the rigidity and order of phosphatidyl choline bilayers in opposite directions. Cholesterol increases orientation and decreases the fluidity of the membrane up to a certain point, while water will disorient an ESR spin label and seems to decrease the thickness of the bilayer (22, 23). Insertion of protein into a synthetic phospholipid bilayer causes an increase in the order parameter of phospholipids (40, 41, 45), or a decrease in the fluidity.

It has also been demonstrated that on a phosphatidylcholine (PC) and phosphatidylserine (PS) membrane, calcium ion causes aggregation of the PS molecules and a remarkable increase in membrane rigidity (21, 46, 47). There is actually a calcium-induced phase separation, also observed with Ba^{++} and Sr^{++}, which is evident from the exchange-broadening in the ESR spectra of PS-PC membranes. There is a rapid, reversible aggregation of PS bridged by Ca^{++} chelation and a fluid phase of PC which can be reversed or attenuated by the presence of Mg^{++} or tetracaine, which is a local anesthetic (48).

Previous studies have indicated that intracellular calcium in human erythrocytes is also a determinant of cellular size, shape, transport of cations, and cell fragility (49-55). Incubation of erythrocyte ghosts and whole blood cells with increasing concentrations of calcium ion causes both gross morphological alteration of the membrane as well as differences in the electrophoretic migratory properties of the membrane proteins. Changes in morphology include deviation from the normal biconcave discoid shape of the circulating erythrocyte

and the appearance of spicules on the surface of the resultant sphere (56, 57). There are also concomitant changes in protein aggregation as noted by freeze-fracture electron microscopy (58). Changes in cellular volume of calcium-treated ghosts seem to be accompanied by a decrease in passive permeability (59) and deformability (60, 61). This is possibly due to changes in the physical state of certain proteins in the erythrocyte membrane (58, 60-63). Bulk water transport is not affected by Ca^{++} concentrations up to 1.0 mM, and the presence of Ca^{++} preserves the normal impermeability to choline, sucrose, Na^{+}, and inulin. Mg^{++} protects the cell from Ca^{++} damage up to 0.3 mM (48).

The aggregation of PS in synthetic bilayers would logically affect the environment of any protein present, and it might be expected that this would occur in both erythrocytes and isolated ghost membranes as well (47). Indeed, this appears to be the case. The mechanism of Ca^{++} action on the membrane is still largely unknown. If, in the circulating erythrocyte, there is a method for concentration of internal calcium within the cell such that such alterations in the lipid and protein components of the membrane occur, the increase in membrane rigidity might initiate removal of these cells from circulation by the microcirculatory system. The decrease in volume might not be sufficient to offset the loss of deformability, and such cells would be trapped in the capillary beds of the spleen, hence removed. This is a possible "self-destruct" method for removal of aged cells. By examining the changes in fluidity, polarity and order within the membrane, we may be able to gain some insight into the degree of alteration of these parameters with a given calcium ion concentration.

We have used stearic acid labels to examine a decrease in viscosity in the lipid portion of membranes of erythrocyte ghosts arising from incubation with increasing concentrations of calcium (0-30mM). We have also looked at the effects of calcium concentrations of 0-15mM on protein in the membranes using 4-maleimido-2, 2, 6, 6-tetramethyl-piperidinooxyl which is known to covalently bond with free sulfhydryl groups and ε-amino groups of lysine.

CHAPTER II

METHODS AND MATERIALS

All spin labels were obtained from Syva Associates, Palo Alto, California. There were four labels used in this series of experiments: 2-(14-carboxytetradecyl)-2-ethyl-4,4-dimethyl-3-oxizolidinyloxyl (16 NMS), 2-(10-carboxydecyl)-2-hexyl-4,4-dimethyl-3-oxizolidinyloxyl (12 NMS), 2-(3-carboxypropyl)-2-tridecyl-4,4-dimethyl-3-oxizolidinyloxyl (5 NMS), and 4-maleimido-2,2,6,6,-tetramethylpiperidinooxyl (MSL). The structures of the labels are given in Fig. 4.

The stearic acid labels were prepared for incorporation by a variation of the method of Landsberger, et al. (64), which consists of dissolving 10 mg of each label in just enough CCl_4 to take it into solution in a 25 ml Erlenmeyer flask. The resultant solution was pale yellow and cloudy. The CCl_4 was evaporated with a gentle stream of nitrogen, leaving a thin film coating the surface of the flask. A 5% aqueous solution of fat-free bovine serum albumin (BSA) was prepared, 10 ml of which was added to the flask. The flask was covered and allowed to stir overnight (12-14 hours) at room temperature to insure adsorption to the BSA. Sample spectra were run to make sure the label in each case had been adsorbed by BSA.

The erythrocytes and erythrocyte ghosts were prepared from fresh blood obtained from the Dallas Blood Bank. Whole red blood cells were washed three times in 10 mM Tris buffer which was 0.154 M in NaCl at

pH 7.4. The buffy coat and debris were removed by aspiration. Both erythrocytes and ghosts were labelled both in salinized 10 mM Tris buffer (pH 7.4) and in isotonic phosphate buffer (pH 6.8) to insure that no change in the labelling occurred due to a change in the buffer system. For the stearic acid labels, the ghost membranes were prepared in Tris buffer as described below. Each sample consisted of 1 ml packed cells which had been resuspended in 10 ml of 10 mM Tris buffer at 4°C. Increasing aliquots of 0.05 M $CaCl_2$ in 10 mM Tris were added to each sample except the control to give a concentration range of 0-30 mM Ca^{++}. The tubes were gently shaken to prevent high localized concentration of Ca^{++} and allowed to incubate at 37° for thirty minutes. The cells were then centrifuged at 7500-8000 rpm for 15 minutes at 4°C and the supernatant was aspirated off. Hemolysis in 10 mM Tris was again performed for one hour at 4°C. (This step was eventually found to be unnecessary and was eliminated.) Membranes were then washed essentially free of hemoglobin and centrifuged to a pellet. The membranes showed a tendency to retain hemoglobin with increasing Ca^{++}, as evidenced by the pinkish color of the membrane pellets and the increase in intensity of the hemoglobin band on electrophoresis. Protein determinations by the method of Lowry (65) were run on each set of samples and indicated that there was 3-5 mg/ml protein per sample. Cholesterol determinations (66) were also run to further confirm the above analysis. Incubation of 0.5 ml packed membranes with 0.5 ml spin label solution was allowed to proceed for six hours at room temperature. This incubation time seemed to be essential in order to get significant labelling of the ghosts. Whole erythorocytes, both fresh and aged,

were labelled in the same manner, but all hemolysis steps were omitted. All samples were occasionally shaken during incubation with the label. The samples were then centrifuged and the supernatants were carefully removed and monitored for excess label. The cells and/or ghosts were carefully washed free of excess label with buffer and resuspended in 0.5 ml buffer.

The electron spin resonance spectra were obtained on an electron spin resonance spectrophotometer constructed in the Physics Department of Oklahoma State University. This instrument is composed of the following components:

Varian 100 KHz field modulation and control unit V4560

Varian V4531 rectangular cavity

Varian V153/6315 reflex klystron tube (90 Mwatts)

Varian V4007-1 electromagnet

Varian V2200 regulated power supply

Varian E-248-1 aqueous solution sample cell.

This is, then, an X-band spectrophotometer utilizing 100 KC modulation and phase-sensitive detection, probably roughly equivalent to a Varian E-3, but much more amenable to modification. The modulation and control unit is applied to signal filtering and phase-sensitive detection for a rectangular microwave resonant cavity. The loss of microwave energy due to the polarity of water molecules is a major problem with aqueous samples. In order to minimize this effect, a Varian E-248 aqueous solution sample cell was used. It enables accurate positioning of the aqueous sample in the planar region of minimum electric field intensity.

Preparation of samples for examination of protein with the MSL label was essentially the same insofar as the Ca^{++} incubations are concerned. However, once the pellet had been spun down, the membranes were washed thoroughly with a 10 mM phosphate buffer, 0.154 M in NaCl, pH 7.4. The MSL label solution was made in phosphate buffer which was 5 mM in NaCl and KCl at pH 6.8. The concentration was adjusted so that there was 1.8×10^{-3} mM label for every 1.6-1.5 mg/ml protein. This procedure was essentially the same as that described by Schneider and Smith (67), except that it was not necessary to preserve ATPase activity. The ghost membranes were allowed to incubate in the label solution for three hours at room temperature. The membranes were washed free of excess label and spectra were run on both samples and supernatants.

Ghosts prepared as described above were solubilized in 1.3% SDS in 0.1 M phosphate (pH 7.8) and 1% mercaptoethanol at room temperature as described by Carraway et al. (62), and subjected to electrophoresis on 5% polyacrylamide gels in 0.1% SDS (62, 68, 69). All gels were stained with Coomassie blue by the procedure of Fairbanks et al. (70). In all cases, the aggregation phenomenon described by Carraway et al. (62, 63) was observed. Whole erythrocytes which were labelled in the two different buffer systems were not subjected to electrophoresis.

CHAPTER III

RESULTS

Membrane models and membrane systems from various sources may be examined with ESR by:

1. Non-covalent labeling.
2. Covalent linkage to protein components.
3. Attachment to lipid components.

We have used stearic acid labels to examine changes in properties in the membranes of erythrocyte ghosts arising from incubation with increasing concentrations of Ca^{++} (0-30 mM). We have also looked at the effects of the same range of Ca^{++} concentrations on protein in the membranes, using 4-maleimido-2,2,6,6-tetramethylpiperidinooxyl. The deliberate variation in the position of the nitroxide label on the hydrocarbon chain of the three stearic acid labels (Fig. 4) enables the investigator to probe the phospholipid bilayer at different levels. This is reasonable since Ca^{++} can have an effect on both the polar and apolar regions of the membrane, though the effect on the polar region would be expected to be greater.

Incubations of fresh and aged whole erythrocytes as well as ghosts prepared from each source were carried out in both phosphate and Tris buffer systems to insure that there was no change in the ESR spectrum due to a change in buffer. There was no observable change between membrane fluidity as measured by ESR between aged erythrocytes and the

Figure 4. Structures of Pertinent Spin Labels

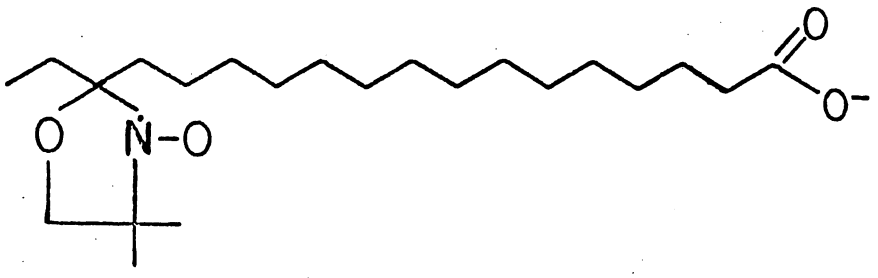

16-NITROXYMETHYL STEARATE
(16 NMS)

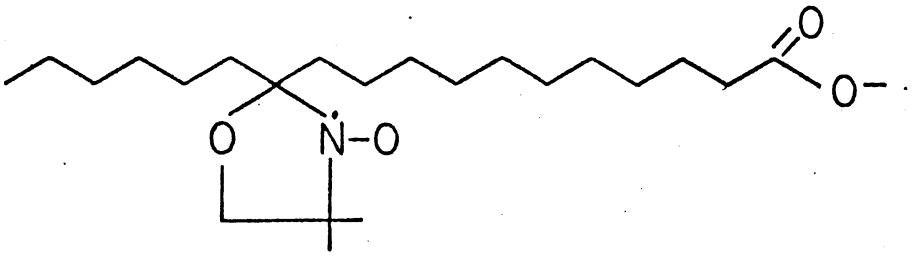

12-NITROXYMETHYL STEARATE
(12 NMS)

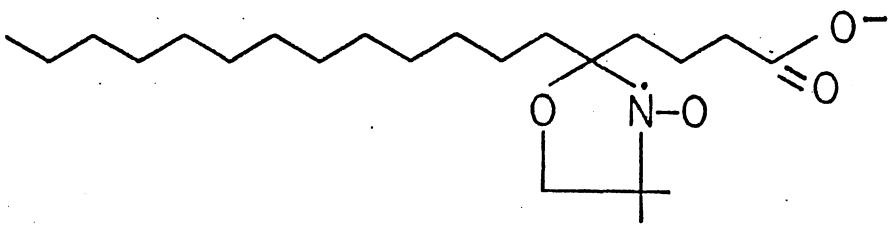

5-NITROXYMETHYL STEARATE
(5 NMS)

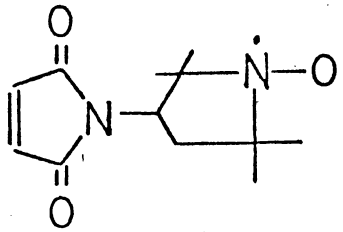

MALEIMIDE SPIN LABEL
(MSL)

ghosts prepared from aged blood, nor between fresh erythrocytes and ghosts (Fig. 5) prepared therefrom. There was, however, a difference in the amount of label taken up in that the erythrocytes did not label as well as ghosts in either case. This implies a greater accessibility of the lipid portion of the membrane to the spin label. From the spectra obtained, there is no observable change in the lipid phase of the intact membrane as compared with ghost membranes within the limits of detectability, which confirms the observations of Landsberger et al. (64). However, there are differences between aged and fresh cells, as indicated by a shift in $2T_{||}'$ (Fig. 6). There is an increased rigidity in the membranes of the aged cells, similar to but not as marked as that observed with calcium-incubated cells. Further, it is known that the calcium effect is not seen with aged blood, indicating that perhaps there is already some change at the surface of the membrane which prevents uptake of calcium during hemolysis.

When the three stearic acid labels, 16 NMS, 12 NMS, and 5 NMS, are incorporated into membranes from fresh blood treated with Ca^{++} during hemolysis there is in all cases a steadily decreasing field separation between high and low field peaks with increasing concentrations of calcium. This can be interpreted as a result of a decrease of the effective $T_{||}'$, implying a decrease in order and an increase in fluidity. The changes in $T_{||}'$ range from about 1.5 Gauss in the labels designated 5 NMS and 16 NMS to about 5.0 Gauss in 12 NMS, as indicated by Tables I through III. The 12 NMS probe will be discussed in more detail since it seemed to give the most information involving changes in the structure of the membrane. With this probe, the change in $2T_{||}$ with increasing concentrations of calcium (0-30 mM) is 7.80 Gauss.

Figure 5. Spectra of Spin Labels Incorporated into Normal RBC Ghosts

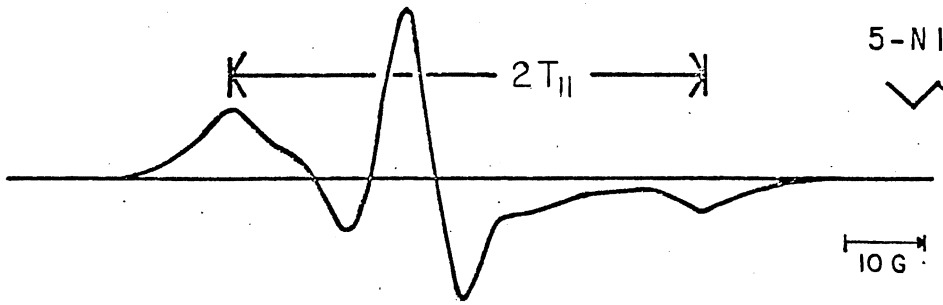

5-NITROXYMETHYL STEARATE (5 NMS)

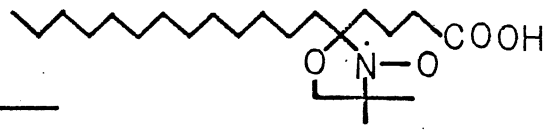

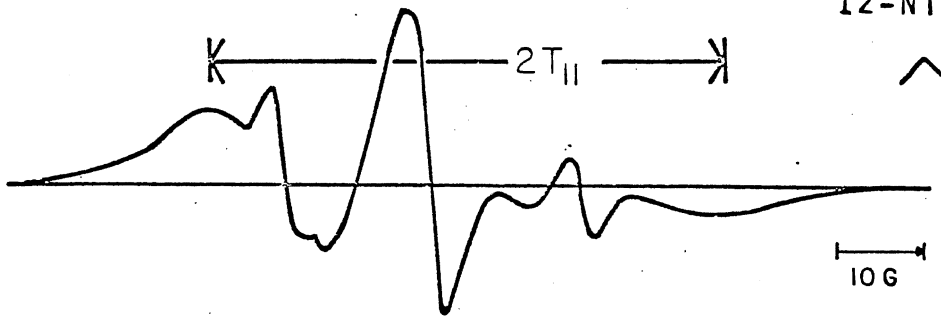

12-NITROXYMETHYL STEARATE (12 NMS)

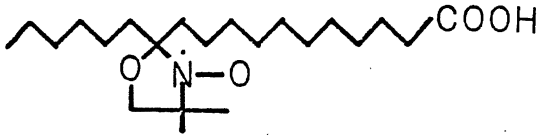

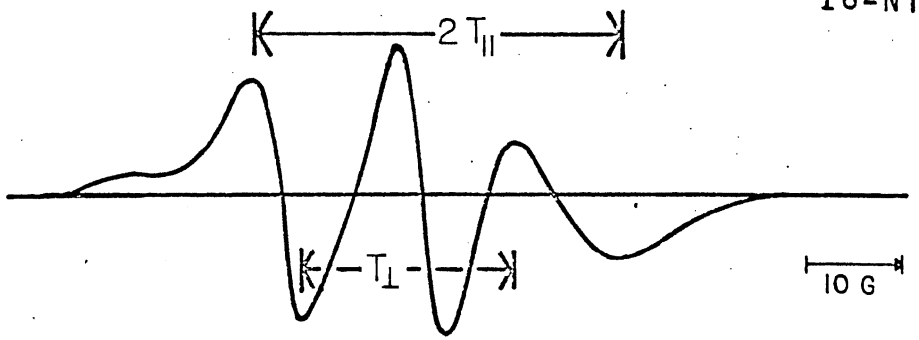

16-NITROXYMETHYL STEARATE (16 NMS)

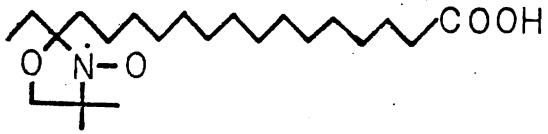

Figure 6. Comparison of ESR Spectra With 5 NMS of Fresh and Aged Erythrocytes Suspended in Both Tris and Phosphate Buffer Systems

Over lay of fresh cells in tris and aged cells in tris

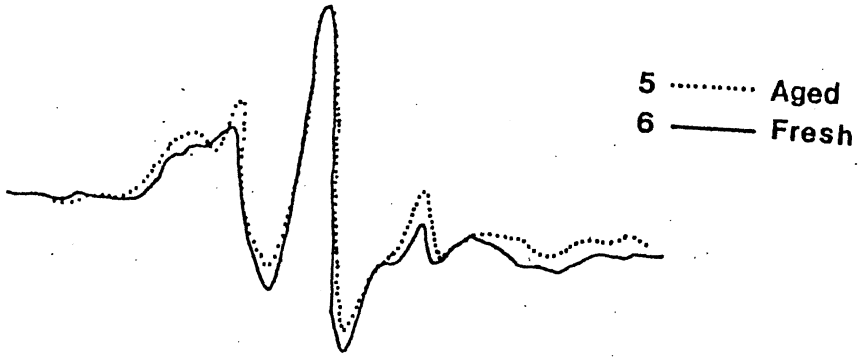

Over lay of fresh cells in tris and aged cells in PO_4

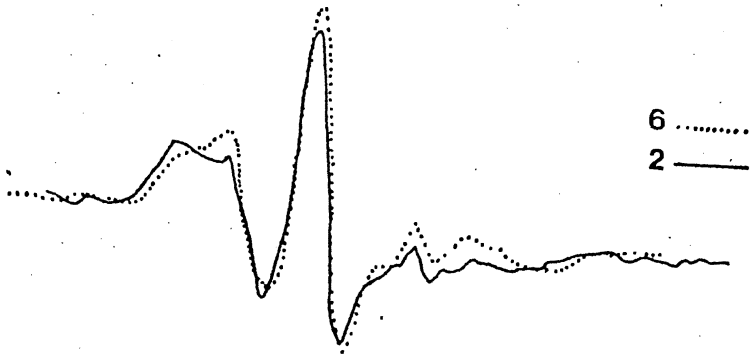

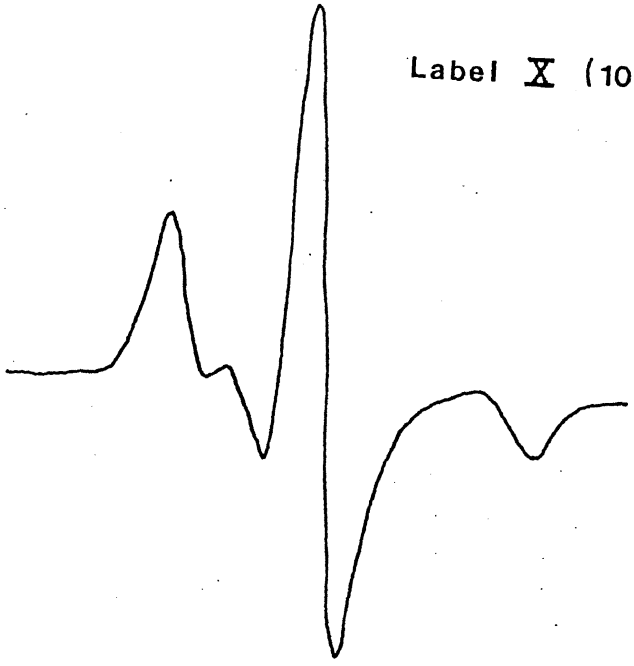

This indicates a very definite decrease in the viscosity of the environment of the nitroxide in this particular region of the membrane (Table I). There is also a decrease in $2T_{||}'$ with the 16 NMS probe, though this change seems to be less marked at first glance (Table II). However, the concentrations monitored with this probe ranged only up to 3.75 mM, and it is significant to note that the largest change in $2T_{||}'$ with the other probes is present in this same Ca^{2+} range. The decrease in $2T_{||}'$ in Gauss over the same concentrations of Ca^{++} for 12 NMS (4.50 G) is roughly twice that of the decrease in $2T_{||}'$ for 16 NMS (2.20 G). Looking at the $2T_{||}'$ values for 5 NMS, there is an even smaller change in $2T_{||}'$ (1.5 G) in going from 0 to 30 mM Ca^{++}. Table III shows values from 0 to 15 mM Ca^{++}, after which there was no further change observed within the limits of our detection system. The shift in fields in the range 0 to 3.75 mM is less than 1 G.

As discussed in the Introduction, the anisotropic N^{14} hyperfine coupling constant, a_n, can be calculated from measurements of $T_{||}'$ and $T_{\perp}'$ by the equation:

$$a_n = \frac{1}{3}(2T_{\perp}' - T_{||}').$$

This coupling constant shows a small dependence upon the polarity of the given solvent, and it follows that it will also show a dependence on the polarity of the environment of the nitroxide in the membrane (Tables I-III). In the case of the label 12 NMS, the coupling constant does show a definite tendency toward a decrease (1.04 G) in the polarity of the environment as shown in Table I, but only up to Ca^{++} concentrations of about 2.5 mM. The a_n values appear nearly constant with Ca^{2+} concentrations increasing above 2.5 mM, though a slight trend is

TABLE I

12 NMS SPIN PROBE IN ERYTHROCYTE GHOSTS

(Ca^{++}) mM	$2T_{11}'$	T_1'	$2T_1'$	T_1'	ΔT	a_N	S
0	57.80	28.90	18.02	9.01	20.89	15.81	0.703
0.50	57.80	28.90	18.02	9.01	20.89	15.81	0.703
0.75	56.50	28.25	18.02	9.01	19.24	15.26	0.698
1.00	56.50	28.50	18.02	9.01	19.24	15.26	0.698
1.50	54.30	28.25	18.20	9.10	18.05	14.96	0.698
2.50	53.60	26.80	18.36	9.18	17.62	14.90	0.655
5.00	53.00	26.50	18.72	9.36	17.14	14.92	0.637
12.50	51.80	25.90	18.92	9.46	16.44	14.79	0.615
25.00	50.10	25.01	19.44	9.72	15.38	14.69	0.581
30.00	50.00	25.00	19.76	9.88	15.12	14.77	0.567

Incubation of erythrocyte ghosts with Ca^{++} followed by labelling with the probe 12 NMS. The a_N values were calculated as follows:

$$a_N = \frac{1}{3}(2T_1' + T_{11}').$$

S values were calculated from the following relationship:

$$S = \left(\frac{T_{11}' - T_1'}{T_{11_{XL}} - T_{1_{XL}}}\right)\left(\frac{a_{N_{XL}}}{a_N'}\right).$$

TABLE II

16 NMS SPIN PROBE IN ERYTHROCYTE GHOSTS

(Ca^{++}) mM	$2T_{\parallel}'$	$T_{\parallel}'$	$2T_{\perp}'$	$T_{\perp}'$	$\Delta T'$	a_N	S'
0	37.40	18.70	20.96	10.50	8.20	13.20	0.277
0.5	37.40	18.70	20.96	10.50	8.20	13.20	0.277
1.0	36.80	18.40	20.92	10.50	7.90	13.11	0.259
2.0	36.30	18.20	20.71	10.50	7.70	13.00	0.244
2.5	35.90	18.00	20.90	10.50	7.50	13.00	0.232
3.75	35.30	17.70	20.90	10.50	7.20	12.90	0.214

TABLE III

5 NMS SPIN PROBE IN ERYTHROCYTE GHOSTS

(Ca^{++}) mM	$2T'_{11}$	T'_{11}	$2T'_{1}$	T'_{1}	ΔT	a_N	S
0	58.85	29.43	18.36	9.18	20.25	15.93	0.703
1.00	58.20	29.10	18.36	9.18	19.92	15.82	0.697
2.00	58.20	29.10	18.36	9.18	19.92	15.82	0.697
4.00	58.00	29.00	18.80	9.40	19.60	15.93	0.681
6.00	57.60	28.80	18.90	9.45	19.35	15.90	0.673
7.50	57.40	28.70	19.30	9.65	19.05	16.00	0.659
15.00	57.30	28.65	19.60	9.80	18.85	16.08	0.649
15.00	No further apparent change						

toward decreasing polarity. With the 16 NMS probe, there is a less drastic change in a_n, even considering the whole range from 0 to 30 mM, in which a_n becomes essentially constant at a concentration of 4.0 mM. The trend is toward a decrease in polarity, but possibly within the limits of experimental error; it is more practical to say that there is little detectable change. In the case of 5 NMS, a trend for a_n cannot readily be assigned.

The order parameter, S, which is ultimately dependent upon the measurement of $2T_{||}'$ and $T_{\perp}'$ from the individual spectra as shown in Fig. 6, may be calculated from Equation (29):

$$S = \left(\frac{\Delta T}{T_{||xL} - T_{\perp xL}}\right)\left(\frac{a_{nxL}}{a_n'}\right)$$

Adequate justification for use of the correction factor derived from crystalline cholestane in a cholesterol chloride preparation is given by several workers (16, 25, 33). The values used for $T_{||}$ and $T_{\perp}$ are taken from McConnell et al. (16), as are the values for a_{nxL}. The order parameter decreases steadily with increasing concentrations of Ca^{++}, indicating an increase in the fluidity of the membrane as shown in Tables I through III. There is a second method for calculation of order parameters as given by Equation (28):

$$S' = \frac{1}{2}\left(3\langle\cos^2\theta\rangle - 1\right)$$

where $\cos^2\theta$ is the square of the cosine of the mean angular deviation. The order parameters are nonidentical, but are related, since the following obtains:

$$\cos^2\theta = \gamma^2 = \frac{(2T_{||}')(1.4) - 16}{70} \qquad (31)$$

$2T_{||}'$ values became extremely difficult to measure in the range of 4 to 30 mM, no further data is presented on this probe. It is, however, significant to note that there is quite a difference in values of 5 NMS as compared with 16 NMS even at 0 mM calcium. There is an angle of roughly 13-14° with the 5 NMS label. Though this value varies slightly from run to run, the change in θ with the change in Ca^{++} is relatively constant at about 4°. Examination of θ for 16 NMS indicates that the deviation of the long axis from orthogonality is quite large (7.7°) over the very small concentration range investigated (0-3.75 mM). Also, the angle itself is more than twice that of the 5 NMS label, ranging from 38.7° to 46.4° in 0 to 3.75 mM calcium. This indicates that this label has a large degree of motional freedom in the absence of calcium, and that the mobility is increased in the presence of even low concentrations of calcium. The largest variation, however, is with the 12 NMS label which shows an increase in mean angular deviation of 13°2' over the concentration range 0 to 30 mM. More significant is the fact that most of this variation (8°45') occurs between 0 to 5 mM. The importance of this becomes more obvious when considered in conjunction with the electrophoretic data. When erythrocytes are incubated with calcium in a hemolyzing buffer at 4°C and subsequently resealed, there is an irreversible aggregation of protein beginning at 1 mM Ca^{++}. This aggregate is not dissociable by SDS and appears at the top of the gels. These observations that the fluidity of the lipid bilayer changes on incubation with increasing concentrations of calcium augments the suggestion by Carraway et al. (62), that a rather extensive reorganization of the membrane occurs. It is obvious from the above data that the lipid bilayer is also involved in these membrane alterations.

where the factor 1.4 is the conversion factor from Gauss to MHz. Though the values obtained are nonidentical, the trend is definitely the same in that the order parameter in either case decreases for all three stearic acid labels. A comparison between both S and S' for these labels is given in Table IV.

The mean angular deviation, which is indicative of mobility of the nitroxide with respect to the long axis of the fatty acid chain, is of particular interest in cases where the other parameters discussed above do not show much change (Table V). Since the fatty acid chain will try to align itself orthogonal to the surface of the membrane, when there is motional freedom in an applied field, the path described by the label with respect to the membrane will be conical (Fig. 7). The deviation of the axis of the fatty acid chain from orthogonality is measured by the angle θ. In the case of the label 5 NMS, though there are measurable differences in $2T_{||}'$ and $T_{\perp}'$, these are much less noteworthy than with the 12 NMS label. This is also true of the a_n and S values. The mean angular deviation, on the other hand, does show an increase of almost 4° with increasing calcium concentration in the range 0-15 mM. When plotted as a function of the change in calcium, the increase in θ appears at first examination to be linear. However, when θ^2 is plotted versus increasing calcium concentration, the resulting straight line indicates that the first plot is actually a gently curving parabola with the maximum inflection point between 0-5 mM calcium (Fig. 8). With the 12 NMS label, the graph of θ versus calcium concentration is sigmoidal with the major change in slope lying between 2-10 mM Ca^{++} (Fig. 9). For 16 NMS, it would appear that the curve may have been sigmoidal (Fig. 9) over a larger concentration range, but since the

TABLE IV

ORDER PARAMETERS S AND S' FOR STEARIC ACID SPIN LABELS

16NMS			12NMS			5NMS		
Ca^{++} in mM/ml Packed Cells	S	S'	Ca^{++} in mM/ml Packed Cells	S	S'	Ca^{++} in mM/ml Packed Cells	S	S'
0	.1335	.277	0	.730	.8911	0	.7040	.9226
0.50	.1335	.277	1.00	.698	.8521	1.00	.6972	.9021
0.75	.1295	.259	1.50	.668	.7861	2.00	.6972	.9021
1.00	.1273	.244	2.50	.665	.7651	4.00	.6813	.8967
2.00	.1240	.232	5.00	.637	.7471	6.00	.6739	.8818
3.75	.1199	.214	12.50	.615	.7111	7.50	.6593	.8776
			25.00	.518	.6601	15.00	.6491	.8747
			30.00	.567	.6571			

TABLE V

MEAN ANGULAR DEVIATIONS FOR STEARIC ACID PROBES

16 NMS		12 NMS		5 NMS	
Ca^{++} in mM	θ in degrees	Ca^{++} in mM	θ in degrees	Ca^{++} in mM	θ in degrees
0	38.7	0	15.50	0	13.0
0.50	38.7	1.0	18.40	1.0	14.8
0.75	44.7	1.5	22.40	2.0	14.8
1.00	45.3	2.5	23.30	4.0	15.2
2.00	45.6	5.0	24.25	6.0	16.3
3.75	46.4	12.5	26.10	7.5	16.6
		25.0	28.50	15.0	16.8
		30.0	28.60		

Figure 7. Path Described by Fatty Acid in Motion is Conical

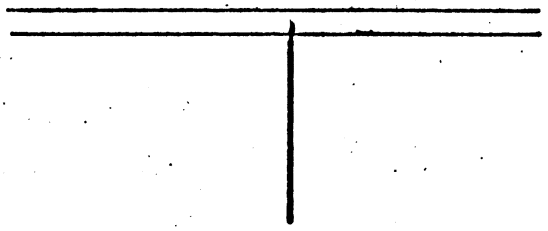

Immobilized

$\theta' = 0$

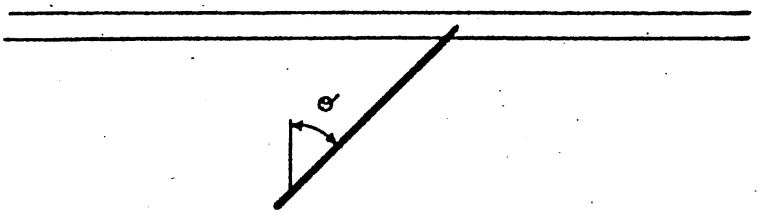

In Motion

θ' has finite value

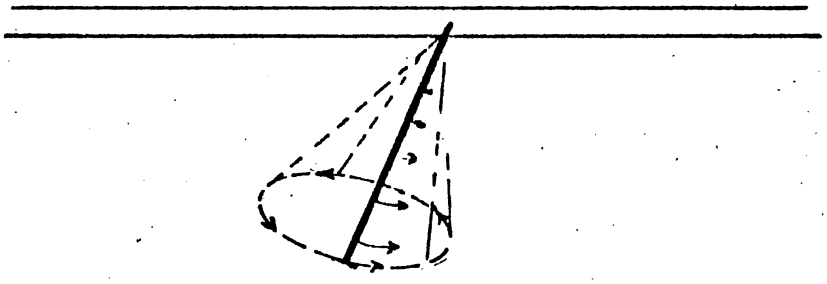

Figure 8. The Effect of Increasing Calcium Concentration on the Mean Angular Deviation With 5 NMS

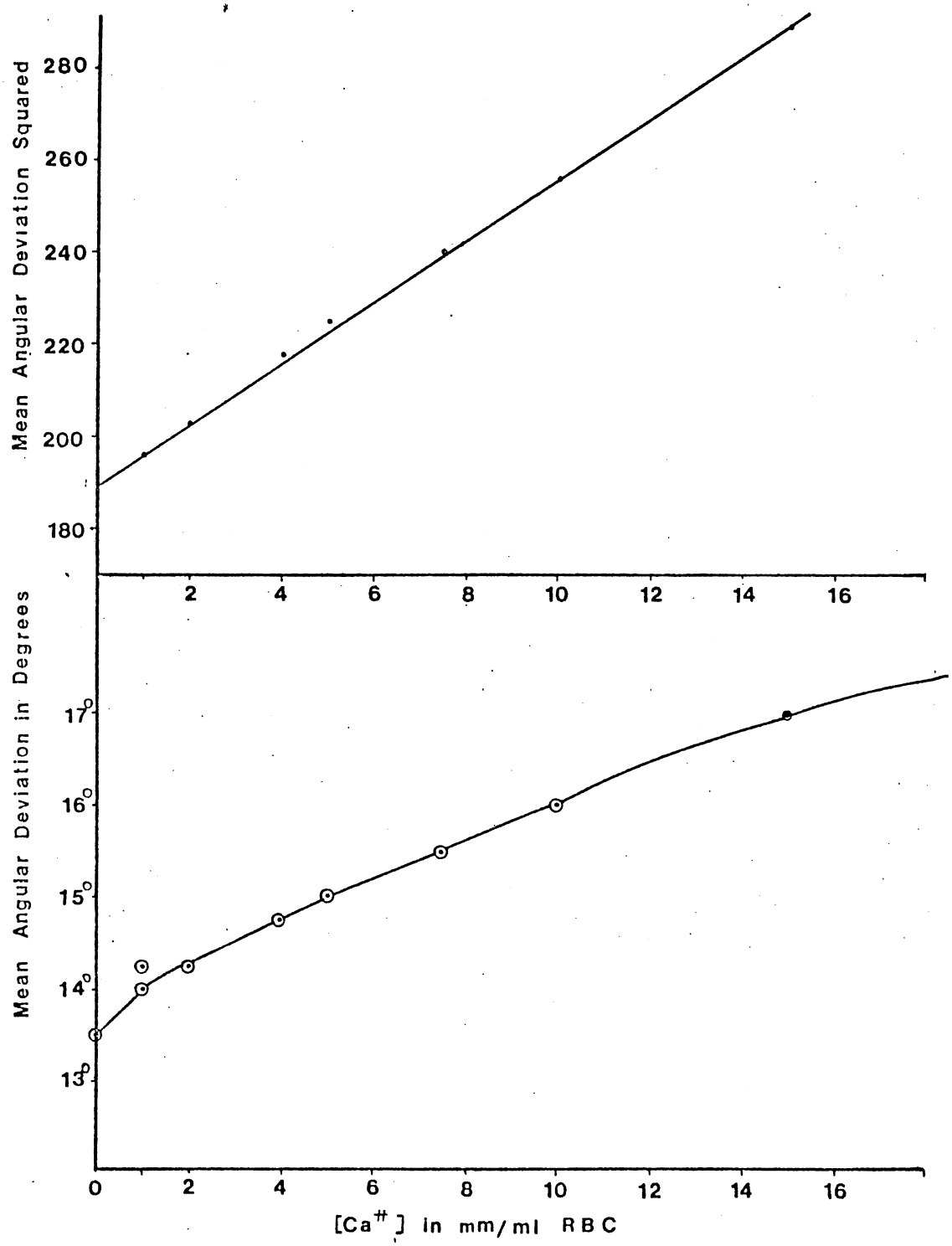
Mean Angular Deviation Squared
280
260
240
220
200
180
2
4
6
8
10
12
14
16
Mean Angular Deviation in Degrees
17°
16°
15°
14°
13°
0
2
4
6
8
10
12
14
16
[Ca++] in mm/ml RBC

Figure 9. The Effect of Increasing Calcium Concentration on the Mean Angular Deviation With 12 and 16 NMS

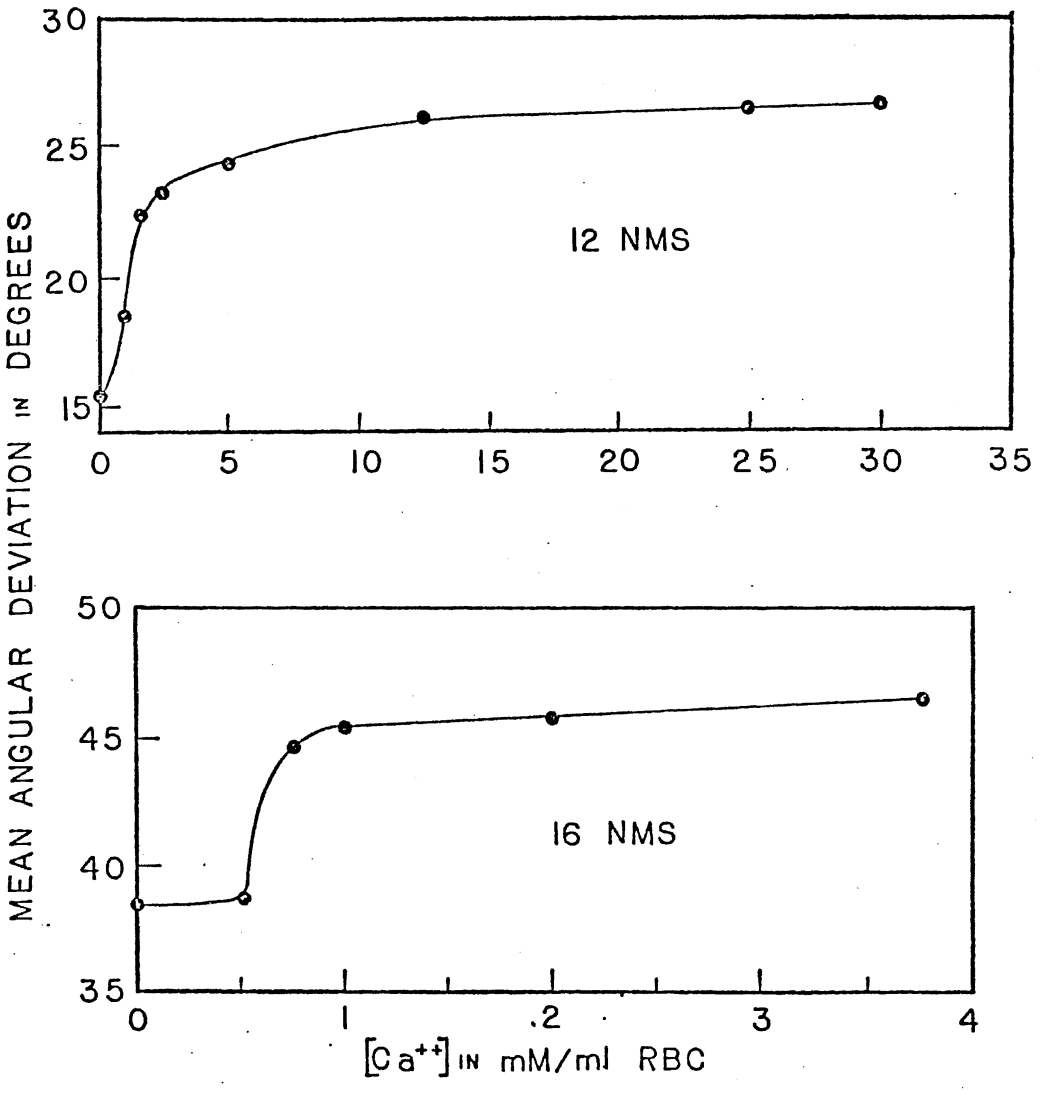
MEAN ANGULAR DEVIATION IN DEGREES
30
25
20
15
12 NMS
0
5
10
15
20
25
30
35
50
45
40
35
16 NMS
0
1
.2
3
4
[Ca++] IN mM/ml RBC

Another method for evaluating order in a membrane system is examination of intensity ratios as Verma has done in his examination of the effects of melittin on erythrocyte membranes (34). In a given spectrum, if we arbitrarily label the first three peaks a, b, and c, the b/c ratio may be calculated. In the case where b/c = 1, there would be perfect ordering about the long axis of the probe. With a decrease in the intensity of b, there is a disordering of the long axis and an increase in mobility. In the examination of the calcium-treated erythrocyte ghosts, there is a decrease in the b/c ratio until a concentration of 2.5-3.0 mM is reached, after which the values are constant.

If the molecular weight of a single ghost membrane were accurately known, then one could calculate the total number of unpaired spins in the sample, hence the concentration of the label would be precisely known. Some work has been done of quantitation of the amount of probe actually taken up by a membrane system (64), and while it may have been feasible to do so with our samples, it would have required more care in measuring the spectra in the supernatants. One can quite easily see, however, changes in the shape of the spectrum attendant with the decrease of $T_{11}^{'}$. Figure 10 shows a large increase in the intensity of the center peak and a decrease in the so-called liquid lines. This may indicate that with increasing concentrations of calcium, there is a greater contribution by the strongly immobilized nitroxide which may be penetrating further into the treated membrane and that there is less exchange of label with the solvent system. However, it is probably more practical to say simply that the intensity increases.

Figure 10. Spectra of Erythrocyte Ghosts in the Presence and Absence of Calcium

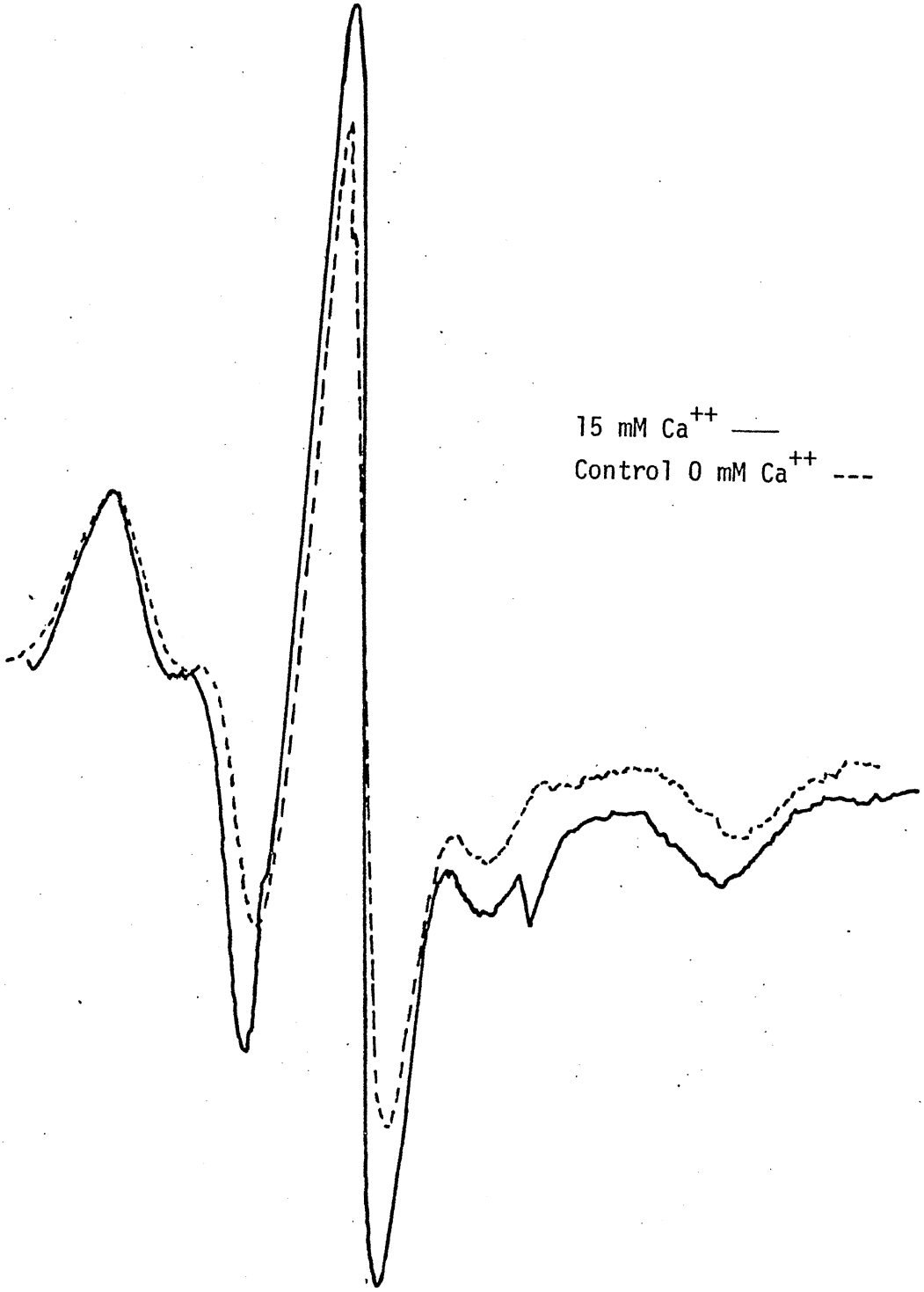
15 mM Ca++
Control 0 mM Ca++

The discussion to this point has centered about changes in the fluidity of the phospholipid components of the membrane. We also conducted preliminary examination of the protein component utilizing the spin label designated MSL (Fig. 4). This probe is known to bind covalently with the free sulfhydryls or with the ε-amino groups (71-74) of the membrane protein (Fig. 11). Since there are potential binding sites on any protein accessible to the label, it is not possible to identify the protein which is labelled by spectrophotometric observation. However, there is always a contribution from weakly immobilized radicals which are bound at the surface and a contribution from strongly immobilized radicals which have penetrated further into the membrane protein. This is true of both the control and the calcium-treated erythrocytes, so any change in the ratio of the strongly (A) to the weakly (B) immobilized contribution to the spectrum (Fig. 12) may be indicative of a change in the state of aggregation of the protein (Fig. 12). A plot of the a/b ratios versus increasing calcium concentration is clearly parabolic (Fig. 13), indicating a change in protein conformation which levels off at about 10 mM. The region of greatest change in slope lies between 1-5 mM calcium concentration. This is in good agreement with the changes observed above with the stearic acid labels and with electrophoretic data. Plots of the order parameter, S, versus calcium concentration for the three stearate labels are shown in Figures 14 and 15 for comparison with Figure 13. Note that the regions of greatest change with respect to calcium concentration are closely comparable. The peak intensity of the center peak also increases but, as with the stearic acid spin probes, no attempt was made at quantitation

Figure 11. Schematic Representation of Incorporation of the Spin Label MSL Into Protein

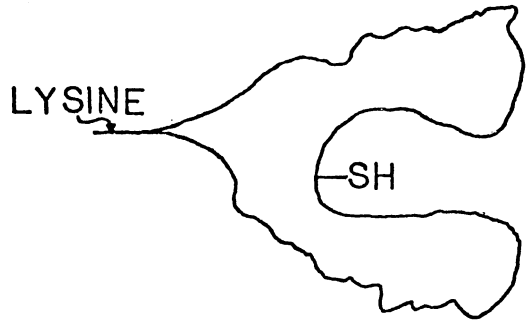

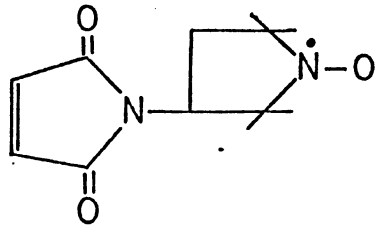

N-(1-OXYL-2,2,5,5-TETRAMETHYLPYRROLIDINYL)-MALEIMIDE

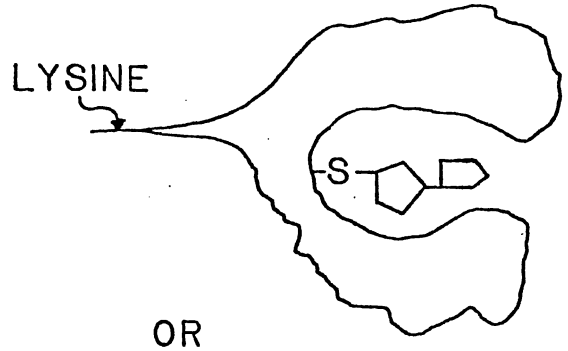

OR

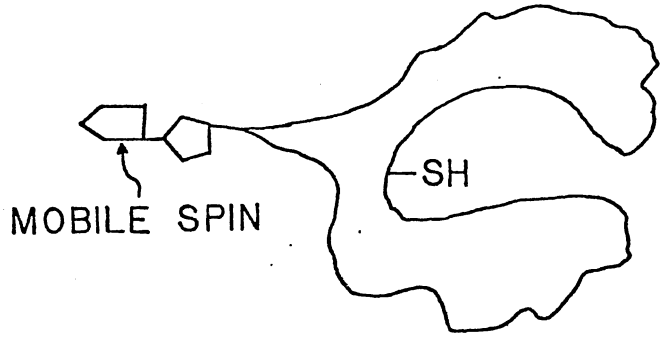

Figure 12. Maleimide Incorporated Into Calcium-Treated Erythrocyte Membranes

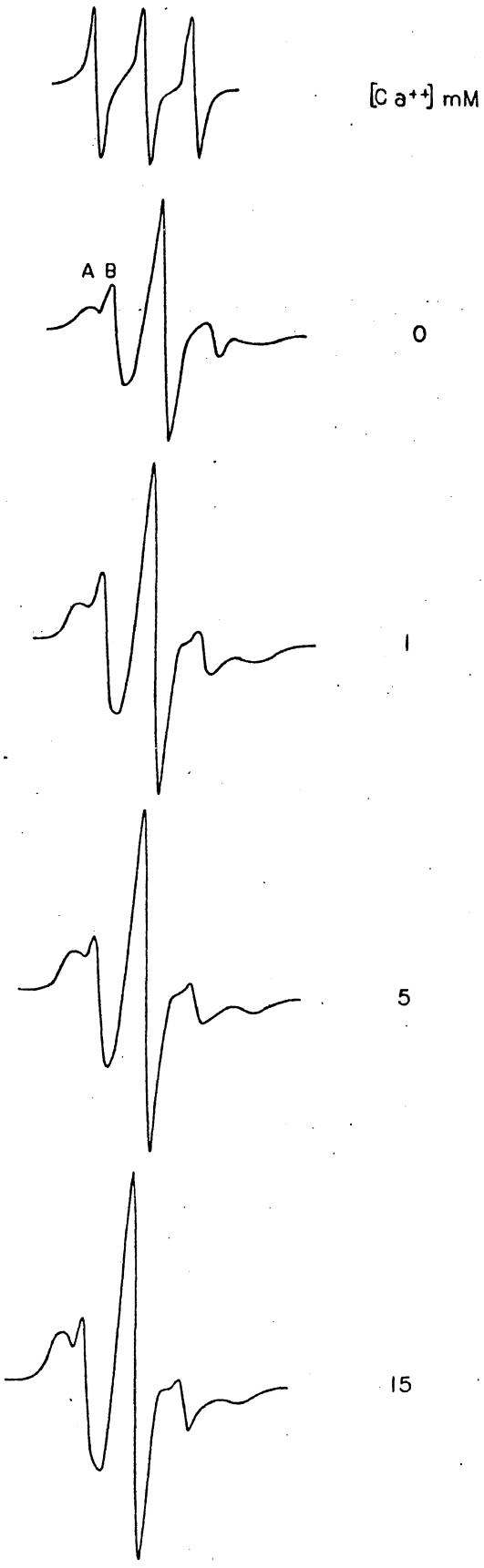
[Ca++] mM
A B
0
1
5
15

Figure 13. Plot of Increasing Calcium Concentration Versus the A/B Ratio

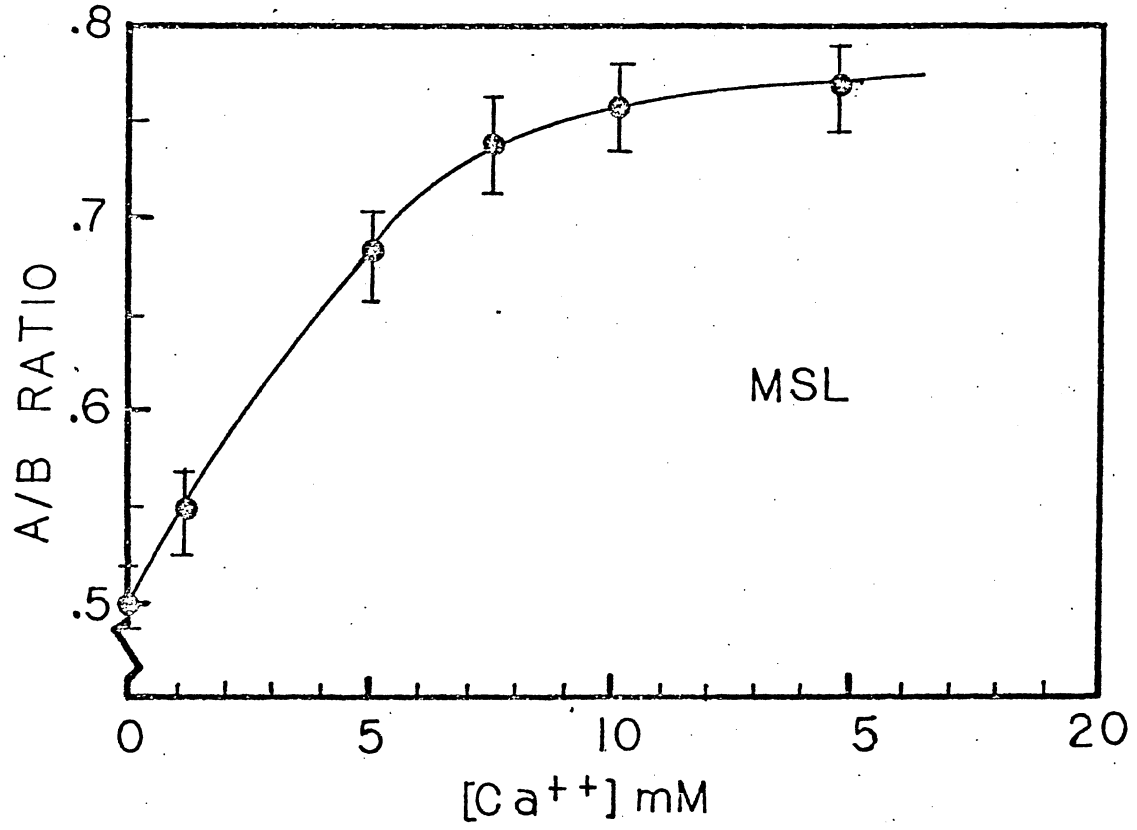
.8
.7
.6
.5
A/B RATIO
MSL
0
5
10
5
20
[Ca++] mM

Figure 14. Variation in Order Parameter, S, With Increasing $[Ca^{++}]$, 16 NMS Label

THE MEAN SQUARE ANGULAR DEVIATION IS DETERMINED FROM $2T_{11}$ BY

$$\overline{\gamma^2} = \frac{2T_{11} - (T_x + T_y)}{2T_z - (T_x + T_y)}.$$

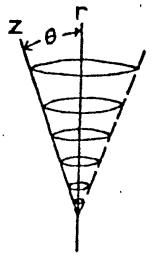

$$\gamma = \cos\theta$$

THE ORDER PARAMETER, S, IS DEFINED IN TERMS OF THE MEAN SQUARE ANGULAR DEVIATION BY

$$S = (3\overline{\gamma^2} - 1)/2.$$

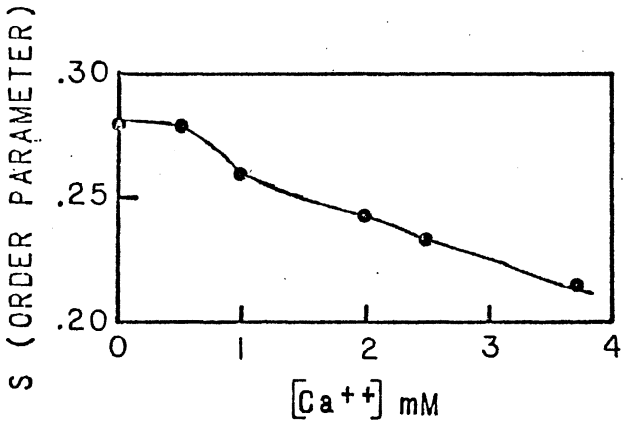

Figure 15. Variation in Order Parameter, S, With Increasing [Ca^{++}], 5 and 12 NMS Labels

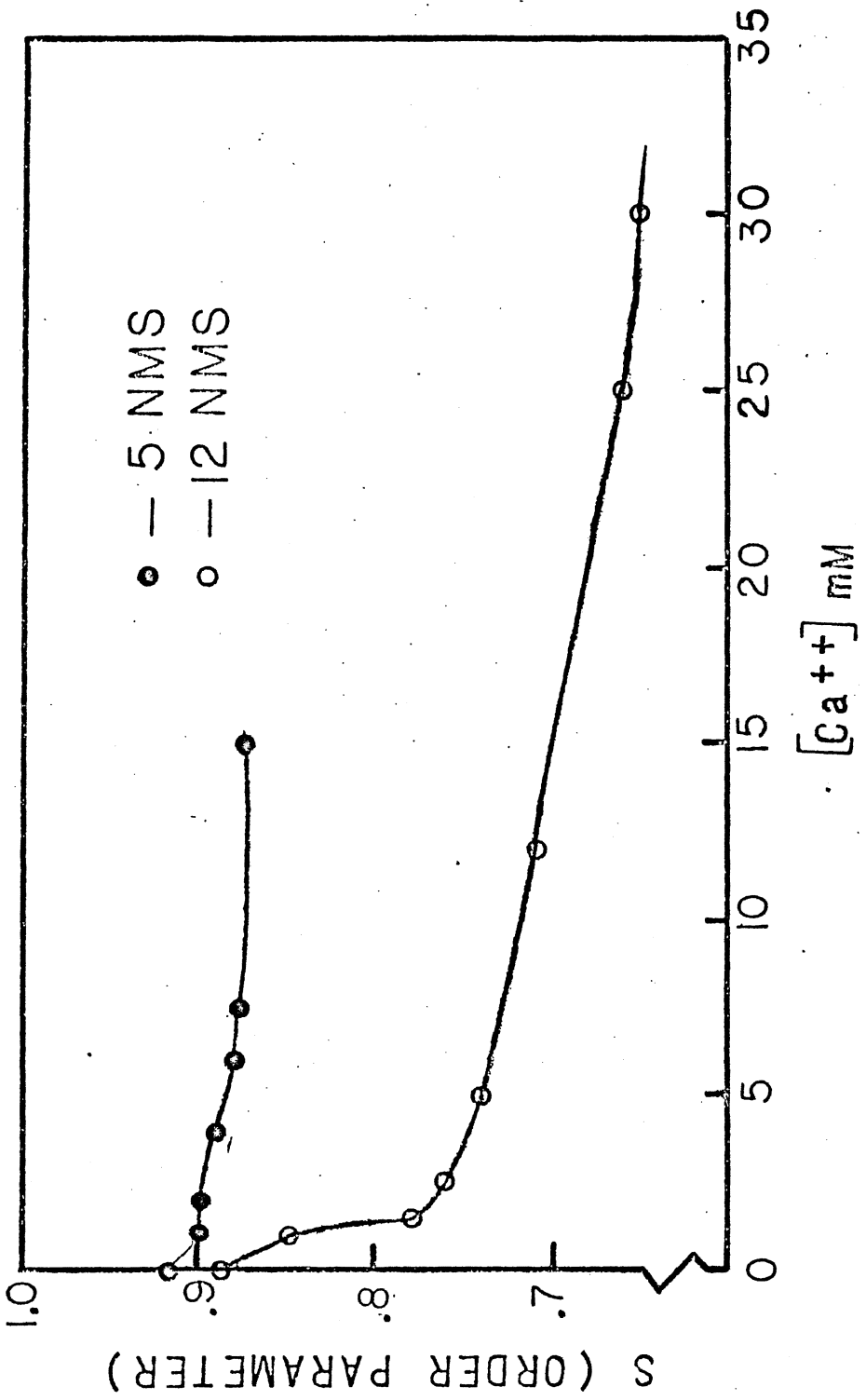
S (ORDER PARAMETER)
1.0
.9
.8
.7
0
5
10
15
20
25
30
35
[Ca++] mM
● — 5 NMS
○ — 12 NMS

of the actual amount of probe bound. Further experimentation in this area has been initiated but will not be reported at this time.

CHAPTER IV

DISCUSSION

It is useful at this point to discuss briefly some assumptions which have been made in reduction of the data. In the original development of parameter calculations, a series of approximations were made by Hubbel and McConnell (37). These were outlined as follows:

1. The effective spin Hamiltonian, $\mathcal{H}'$, has axial symmetry.

2. The line shape for each hyperfine signal is Lorentzian (though this is not always strictly true).

3. The line width for each hyperfine signal is isotropic, but m-dependent where m is the component of the nitrogen nuclear spin in the local field direction at the nucleus.

4. The spatial distribution of the average hyperfine axis in oriented multibilayers is given by:

$$\rho(\vartheta) = \sin\vartheta^{[-(\vartheta-\bar{\vartheta})^2/2\vartheta_o^2]} \tag{32}$$

This is a distribution function for the principle axis, Z', where ϑ is the angle between Z' and $\underline{N}$ which is normal to the planes of the phospholipid bilayers (Fig. 16).

There are a series of further approximations also pertinent to the dependence of the spectra on Eigenvalues of the time-dependent Hamiltonian, $\mathcal{H}'$, and perturbations thereof. These obtain under certain conditions and include considerations that the individual widths

Figure 16. The Axis System Defining the Orientation of the Molecular Z' Axis With Respect to the Magnetic Field Direction H

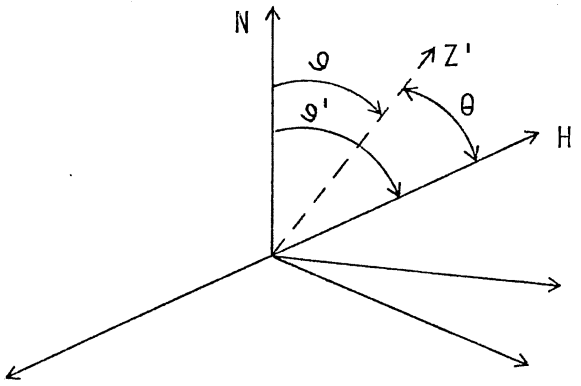

of resonance lines are angular dependent, and that the effective or time-dependent Hamiltonian, $\mathcal{H}'$, does not have axial symmetry in either the g' or T' tensor. The calculated spectra employing the above approximations are very similar to the experimentally observed spectra; therefore, we may assume that the approximations made are valid. The method is, as pointed out in the Introduction, a valuable and sensitive method for examination of biological membranes as well as for synthetic systems.

Assumptions must be made about the labelling of the membrane itself. The spin label may possibly be bound nonspecifically at two or more conformationally different sites on the membrane, and could give rise to both a weakly immobilized and a strongly immobilized contribution to the spectrum. Indeed, Wallach and coworkers (27) have observed that 5 NMS may be complexing with arginine residues as well as interacting with lipids in the membrane. This would render the analysis of these spectra with respect to specific lipid-protein interactions very difficult indeed. It would not, however, alter the

reflection by that label of increased lipid fluidity, since both components are labelled and the hydrophobic binding element is large in any case.

Aged intact erythrocytes, in contrast to fresh intact cells, reflect an increase in the fluidity of the membrane similar to that observed at low calcium concentrations. Indeed, the calcium effect cannot be seen at all with aged cells. There is a difference in the ability of the intact cells in any case to take up label with the stearate labels. This implies some difference in the membranes in the two systems. This is in agreement with the studies of Zwaal et al. (75).

There are differences in the magnitude of changes in T_{11}', which decreases in the presence of increasing $[Ca^{++}]$, with each of the different stearate labels. These are, however, all in the same direction; therefore one may conclude that there is a decrease in the viscosity in the immediate proximity to the label in each instance. This implies that similar changes are occurring at different levels within the lipid component of the membranes. The most significant changes occur between 1-5 mM Ca^{++}, and little change is observed beyond 15 mM. The most useful label for monitoring the process appears to be 12 NMS, since it is sensitive to change over larger concentration ranges.

The order parameters, which are representative of time averages over molecular motions are such that the longer the time involved in averaging, the lower the parameters. The averaging time, in turn, is dependent upon the magnitudes of the anisotropic contributions to the spin Hamiltonian, which involves hyperfine and g-factor interactions.

These have been quantitated for each of the stearate labels. These order parameters, S and S', as shown in Table IV, indicate a decrease in value for each label, hence decreasing order in the lipid portion of the membrane.

The interrelationship between the order parameters and the mean angular deviation has been discussed above. There is an increase in the angles in each instance (Table V), indicating an increase in mobility of the label with increasing calcium concentration. The initial angles vary widely among the three labels, but the trend is the same.

The observed increase in intensity of the center peak of the spectrum implies that the lipid layer becomes increasingly accessible to the stearate labels with increasing calcium concentration. This perhaps indicates that the lipids are less tightly packed.

Data obtained so far with the protein label MSL suggests that there is a conformational change occurring between 1-5 mM Ca^{++}, which is the region of greatest change for the stearate labels as well. This is also the concentration range in which protein aggregation has been observed by Carraway et al. (62, 63). The concentration of 5 mM Ca^{++} brings about irreversible aggregation of membrane protein.

These observations indicate that increasing Ca^{++} concentrations induce a definite decrease in the order of the lipid portion of the membrane and an accompanying conformational change in some as yet unspecified protein component. One might speculate that this could be directly related to the observed phase changes induced by Ca^{++} in synthetic bilayers (47). Since Zwaal (75) has indicated that the outer portion of the erythrocyte membrane consists of predominantly

choline-containing phospholipids, it might behoove us to use labelled phosphatidyl choline as McConnell et al. (76) have done with rabbit sarcoplasmic reticulum. The diffusion constant for lateral diffusion of phospholipids could then be monitored. This is of particular applicability since the sarcoplasma sequesters Ca^{++} from the mycoplasma and an in vitro assay for Ca^{++} uptake was used as a measure of the integrity of spin labelled membranes.

Other protein labels must be employed in order to identify the protein moiety affected by the presence of high Ca^{++} concentrations. Gotto et al. (71, 77) have used two different methods for labelling proteins. The first employed MSL to study lipid-protein interactions in lipoproteins (71). Very little could be said about lipoprotein-protein interactions, though it is significant that very little perturbation of the membrane was observed in the presence of the spin label. The second label was an isothiocyanate nitroxide label. There were both weakly and strongly immobilized sites of attachment. The strongly constrained signal was thought to arise from lipid-protein interaction which reduced the molecular motion of the spin label bound to the protein. There is also an organophosphorus derivative, the method for preparation of which is given by Morrisett et al. (78), which will label serine groups in apolar environments. There are also steroidal nitroxides which may be used (79).

Future studies utilizing this array of labels should enable us to observe the subtle interactions attendant with the observed organizational changes of the protein.

REFERENCES

(1) Slictor, C. P. (1963) Principles of Magnetic Resonance, Harper and Row, New York.

(2) McConnell, H. M. and McFarland, B. G. (1970) Quart. Rev. Biophys., 3, 91.

(3) Jost, P., Waggoner, A. S., and Griffith, C. H., in L. Rothfield (1971) Structure and Function of Biological Membranes, Academic Press, New York, 84.

(4) Fehler, G. (1970) EPR With Application to Selected Problems in Biology, in Les Houches Lectures (1969) Gordon and Breach, New York.

(5) Stone, T. J., Buckman, T., Nordio, P. L., and McConnell, H. M. (1965) Proc. Natl. Acad. Sci. U. S., 54, 1010.

(6) Berliner, L. J. and McConnell, H. M. (1966) Proc. Natl. Acad. Sci. U. S., 55, 708.

(7) Hamilton, C. L. and McConnell, H. M. in A. Rich and N. Davidson (1968) Structural Chemistry and Molecular Biology, W. H. Freeman and Co., San Francisco, 115.

(8) Ogawa, S. and McConnell, H. M. (1967) Proc. Natl. Acad. Sci. U. S., 58, 19.

(9) Smith, I. C. P. (1968) Biochemistry, 7, 745.

(10) Griffith, C. H. and Waggoner, A. S. (1969) Accounts Chem. Res., 2, 17.

(11) Chang, R. (1971) Basic Principles of Spectroscopy, McGraw-Hill, New York.

(12) Freed, J. H. and Fraenkel, G. K. (1963) J. Chem. Phys., 39, 326.

(13) Hudson, A. and Lockhurst, G. R. (1969) Chem. Rev., 69, 191.

(14) Seelig, J. (1973) Separatum Experientia, 29, 509.

(15) Vanin, A. F. and Ruuge, E. K. (1968) Biofizika, 13, 471.

(16) Gaffney, B. J. and McConnell, H. M. (1974) J. Mag. Res., 16, 1.

(17) McConnell, H. M. (1956) J. Chem. Phys., 25, 709.

(18) Kivelson, D. (1964) J. Chem. Phys., 41, 1904.

(19) Sohn, R. and Marinetti, G. U. (1974) Chem. Phys. Lipids, 12, 17.

(20) Seeling, J. (1970) J. Am. Chem. Soc., 92, 3881.

(21) Schnepel, G. H., Hegner, D. and Schummer, U. (1974) Biochim. Biophys. Acta, 367, 67.

(22) Boggs, J. M. and Hsia, J. C. (1972) Biochim. Biophys. Acta, 290, 32.

(23) Hsia, J. C., Long, R. A., Hruska, F. E., and Gesser, H. D. (1972) Biochim. Biophys. Acta, 290, 22.

(24) Seelig, J. and Neiderberger, W. (1974) Biochem., 13, 1585.

(25) Butler, K. W., Tattrie, N. H. and Smith, I. C. P. (1974) Biochim. Biophys. Acta. 363, 351.

(26) Staros, J. V., Haley, B. E. and Richards, F. M. (1974) J. Biol. Chem., 249, 5004.

(27) Wallach, D. F. H., Verma, S. P., Weidekamm, E., and Bieri, V. (1974) Biochim. Biophys. Acta, 356, 68.

(28) Simpkins, H., Panko, E. and Tay, S. (1971) Biochem., 10, 3851.

(29) Waggoner, A. S., Kingzett, T. J., Rottschaefer, S., Griffith, O. H., and Keith, A. D. (1969) Chem. Phys. Lipids, 3, 245.

(30) Landsberger, F. R., Lenard, J., Paxton, J., and Compans, R. W. (1971) Proc. Natl. Acad. Sci. U. S., 68, 2579.

(31) Kaplan, J., Canonico, P. G. and Caspary, W. J. (1973) Proc. Natl. Acad. Sci. U. S., 70, 66.

(32) Swartz, H. M., Bolton, J. R. and Borg, D. C. (1972) Biological Applications of Electron Spin Resonance, Wiley-Interscience, New York.

(33) Butterfield, D. A., Roses, A. D., Cooper, M. L., Appel, S. H., and Chestnut, D. B. (1974) Biochem., 13, 5078.

(34) Verma, S. P., Wallach, D. F. H. and Smith, I. C. P. (1974) Biochim. Biophys. Acta, 345, 129.

(35) Hubbell, W. L. and McConnell, H. M. (1968) Proc. Natl. Acad. Sci. U. S., 61, 12.

(36) Hubbell, W. L. and McConnell, H. M. (1969) Proc. Natl. Acad. Sci. U. S., 64, 20.

(37) Hubbell, W. L. and McConnell, H. M. (1971) J. Am. Chem. Soc., 93, 314.

(38) Simkins, H., Tay, S. and Panko, E. (1971) Biochem., 10, 3579.

(39) Landsberger, F. R., Compans, R. W., Paxton, J. and Lenard, J. (1972) J. Supramol. Struct., 1, 50.

(40) Seelig, J. and Hasselbach, W. (1971) Eur. J. Biochem., 21, 17.

(41) Rottem, S., Hubbell, W. L., Hayflick, L., and McConnell, H. M. (1970) Biochim. Biophys. Acta, 219, 104.

(42) James, R., Branton, D., Wisnieski, B., and Keith, A. (1972) J. Supramol. Struct., 1, 38.

(43) Keith, A. D., Waggoner, A. S. and Griffith, O. H. (1968) Proc. Natl. Acad. Sci. U. S., 61, 819.

(44) Barnett, R. E., Furcht, L. T. and Scott, R. E. (1974) Proc. Natl. Acad. Sci. U. S., 71, 1992.

(45) Hong, K. and Hubbell, W. L. (1972) Proc. Natl. Acad. Sci. U. S., 69, 2617.

(46) Chinishi, S. and Tadanao, I. (1974) Biochem., 13, 881.

(47) Butler, K. W., Dugas, H., Smith, I. C. P., and Schneider, H. (1970) Biochem. Biophys. Res. Comm., 40, 770.

(48) Colombe, B. W. and Macey, R. I. (1974) Biochim. Biophys. Acta, 363, 226.

(49) Hoffman, J. F., Tosteson, D. C. and Whittam, R. (1960) Nature, 185, 186.

(50) Hoffman, J. F. (1962) J. Gen. Physiol., 45, 837.

(51) Hoffman, J. F. (1962) Circulation, 26, 1201.

(52) Palek, J., Kirby, W. A. and Lionetti, F. J. (1971) Am. J. Physiol., 220, 19.

(53) Wins, P. and Schoffeniels, E. (1966) Biochim. Biophys. Acta, 120, 341.

(54) Schatzmann, H. J. (1966) Experientia, 22, 364.

(55) Olson, E. J. and Cazort, R. J. (1969) J. Gen. Physiol., 53, 311.

(56) Dunn, M. J. and Grant, R. (1974) Biochim. Biophys. Acta, 352, 97.

(57) Manery, J. F. (1966) Fed. Proc., 25, 1804.

(58) Barnett, R. E., Furcht, L. T. and Scott, R. E. (1974) Proc. Natl. Acad. Sci. U. S., 71, 1992.

(59) Palek, J., Curby, W. A. and Lionetti, F. J. (1971) Am. J. Physiol., 220, 19.

(60) Weed, R. I. and Chailley, B. (1972) Nouvelle Revue Francaise d'Hematologie, 12, 775.

(61) LaCelle, P. L. (1969) Transfusion, 9, 238.

(62) Triplett, R. B., Wingate, J. M. and Carraway, K. L. (1972) Biochem. Biophys. Res. Comm., 49, 1014.

(63) Carraway, K. L., Triplett, R. B. and Anderson, D. R. Unpublished.

(64) Landsberger, F. R., Paxton, J. and Lenard, J. (1971) Biochim. Biophys. Acta, 266, 1.

(65) Dodge, J. T., Mitchell, C. and Hansan, D. J. (1963) Arch. Biochem. Biophys., 100, 119.

(66) Best, C. H., Lucas, C. C., Patterson, J. H., and Ridout, J. H. (1946) Biochem. J., 40, 338.

(67) Schneider, H. and Smith, I. C. P. (1970) Biochim. Biophys. Acta, 219, 61.

(68) Kobylka, D., Khettry, A., Shin, B. C. and Carraway, K. L. (1972) Arch. Biochem. Biophys., 148, 475.

(69) Carraway, K. L. and Kobylka, D. (1970) Biochim. Biophys. Acta, 219, 238.

(70) Fairbanks, G., Steck, T. L. and Wallach, D. F. H. (1971) Biochem., 10, 2606.

(71) Gotto, A. M., Kon, H. and Birnbaumer, M. E. (1970) Proc. Natl. Acad. Sci. U. S., 65, 145.

(72) Benesch, R. and Benesch, R. E. (1961) J. Biol. Chem., 236, 405.

(73) Sharpless, N. E. and Flavin, M. (1966) Biochem., 5, 2963.

(74) Sandberg, H. E., Bryant, R. G. and Piette, L. H. (1969) Arch. Biochem. Biophys., 133, 144.

(75) Zwall, R. F. A., Roelofsen, B. and Colley, C. M. (1973) Biochim. Biophys. Acta, 300, 159.

(76) Scandella, C. J., Devaux, P. and McConnell, H. M. (1972) Proc. Natl. Acad. Sci. U. S., 69, 2056.

(77) Gotto, A. M. and Kon, H. (1969) Biochem. Biophys. Res. Comm., 37, 444.

(78) Morrisett, J. D., Broomfield, C. A. and Hackley, B. E. (1969) J. Biol. Chem., 244, 5758.

(79) Chambez, E., Defaye, G., Hadjian, A., Martin, P., Ramasseul, R., and Rassat, A. (1971) FBS Letters, 19, 55.

VITA

Dorothy Adams Bertler

Candidate for the Degree of

Master of Science

Thesis: ELECTRON SPIN RESONANCE STUDIES OF CALCIUM-TREATED HUMAN ERYTHROCYTES AND ERYTHROCYTE GHOSTS

Major Field: Biochemistry

Biographical:

Personal Data: Born in Lufkin, Texas, February 7, 1942, the daughter of Lt. Eugene E. and Mrs. Julienne L. Adams.

Education: Graduated from Lufkin Senior High School, Lufkin, Texas, in May, 1958; received Bachelor of Arts degree, May, 1967, from St. Mary's University, San Antonio, Texas; received Master of Science degree, June, 1973, from University of Puget Sound, Tacoma, Washington; completed requirements for the Master of Science degree in Biochemistry at Oklahoma State University in July, 1975.

Professional Experience: Stockroom supervisor and supervisor of teaching assistants, Department of Biology, St. Mary's University, San Antonio, Texas, May, 1967 to June, 1968; Graduate Teaching Assistant/Staff Assistant, Department of Chemistry, University of Puget Sound, Tacoma, Washington, August, 1971 to June, 1973; Research Assistant, Department of Biochemistry, Oklahoma State University, Stillwater, Oklahoma, August, 1973 to present; Teaching Assistant, Department of Chemistry, Oklahoma State University, August, 1974 to present.

Professional Organizations: Member of the American Chemical Society and Phi Lambda Upsilon Honor Society.